Research in Astron. Astrophys. **2010** Vol. **10** No. **5**, 383–414
http://www.raa-journal.org *http://www.iop.org/journals/raa*

Research in Astronomy and Astrophysics

Debris disks: seeing dust, thinking of planetesimals and planets

Alexander V. Krivov

Astrophysical Institute and University Observatory, Friedrich Schiller University Jena, Schillergäßchen 2–3, 07745 Jena, Germany; *krivov@astro.uni-jena.de*

Received 2010 March 5; accepted 2010 March 24

Abstract Debris disks are optically thin, almost gas-free dusty disks observed around a significant fraction of main-sequence stars older than about 10 Myr. Since the circumstellar dust is short-lived, the very existence of these disks is considered as evidence that dust-producing planetesimals are still present in mature systems, in which planets have formed – or failed to form – a long time ago. It is inferred that these planetesimals orbit their host stars at asteroid to Kuiper-belt distances and continually supply fresh dust through mutual collisions. This review outlines observational techniques and results on debris disks, summarizes their essential physics and theoretical models, and then places them into the general context of planetary systems, uncovering interrelations between the disks, dust parent bodies, and planets. It is shown that debris disks can serve as tracers of planetesimals and planets and shed light on the planetesimal and planet formation processes that operated in these systems in the past.

Key words: planetary systems: formation — circumstellar matter

1 INTRODUCTION

An inventory of our own planetary system uncovers its complex architecture. Eight known planets are arranged in two groups, four terrestrial ones and four giants. The main asteroid belt between two groups of planets, terrestrial and giant ones, comprises planetesimals that failed to grow into planets because of the strong perturbations by nearby Jupiter (e.g., Safronov 1969; Wetherill 1980). The Edgeworth-Kuiper Belt (EKB) exterior to Neptune's orbit is built up by planetesimals that did not form planets because the density of the outer solar nebula was too low (e.g., Safronov 1969; Lissauer 1987; Kenyon & Bromley 2008). Both the asteroid belt and the Kuiper belt are heavily sculptured by planets, predominantly by Jupiter and Neptune respectively. Accordingly, they include non-resonant and resonant families, as well as various objects in transient orbits ranging from detached and scattered Kuiper-belt objects through Centaurs to Sun-grazers. Short-period comets, another tangible population of small bodies in the inner solar system, must be genetically related to the Kuiper belt that act as their reservoir (Quinn et al. 1990). Asteroids and short-period comets together are sources of interplanetary dust, observed in the planetary region, although their relative contribution to the dust production remains uncertain (Grün et al. 2001). This complex system structure was likely quite different in the past. It is argued that the giant planets and the Kuiper belt originally formed in a more compact configuration (the "Nice model," Gomes et al. 2005), and that it went through a short-lasting period of dynamical instability, likely explaining the geologically recorded event of the Late Heavy Bombardment (LHB).

Similar to the solar system, planetary systems around other stars are more than the star itself and one or several planets. As Wyatt (2008) pointed out, at the end of the protoplanetary phase, a star is expected to be surrounded by at least one but perhaps all of the following components: various planets from sub-Earth to super-Jupiter size; remnants of the protoplanetary disk, both dust and gas; planetesimal belts in which solids continue to grow; and planetesimal belts, which are being ground down to dust. Indeed, many systems comprise numerous smaller objects, ranging in size presumably from dwarf planets (like Pluto or Ceres) down to dust. Evidence for this comes from observations of the thermal emission and stellar light scattered by that dust. A common umbrella term for all these "sub-planetary" solids is a "debris disk." Debris disks are aftermaths of planet formations in the past, and they formed in the same process as the planets did. Even in mature systems where the planet formation has long been completed, they continue to evolve collisionally and dynamically, are gravitationally sculptured by planets, and the dust they produce through ongoing collisional cascades responds sensitively to electromagnetic and corpuscular radiation of the central star. Hence, debris disks can serve as indicators of invisible small bodies, planets, and even stars, are tracers of their formation and evolution, and represent an important component of planetary systems.

We start by outlining observational techniques and results on debris disks (Sect. 2) and summarizing their essential physics (Sect. 3) and models (Sect. 4). In the subsequent sections, the observational data and their theoretical interpretation are used to draw conclusions about the "dust end" of the size distribution, dust itself (Sect. 5), its parent planetesimals (Sect. 6), planets expected to be present in debris disk systems (Sect. 7), and the entire planetary systems (Sect. 8). Section 9 provides a summary and lists open questions related to debris disk research.

2 OBSERVATIONAL METHODS

2.1 Infrared Excesses

An efficient, and historically the first successful, way of detecting circumstellar dust is infrared (IR) photometry. If dust is present around a star, it comes into thermal equilibrium with the stellar radiation. With equilibrium temperatures of dust orbiting a solar-type star at several tens of AU being typically several tens of Kelvin, dust re-emits the absorbed stellar light at wavelengths of several tens of micrometers, i.e. in the far-IR. As a result, the dust far-IR emission flux may exceed the stellar photospheric flux at the same wavelength by two-three orders of magnitude. The first discovery of this type of excess IR emission around a main-sequence star, namely Vega, was done by the Infrared Astronomical Satellite (IRAS) (Aumann et al. 1984). Since then, IR surveys with IRAS, ISO, Spitzer, and other space-based and ground-based telescopes have shown "the Vega phenomenon" to be common for main-sequence stars. In particular, various photometric surveys of nearby stars have been conducted with the Spitzer Space Telescope. These are the GTO survey of FGK stars (Beichman et al. 2005; Bryden et al. 2006; Beichman et al. 2006), the FEPS Legacy project (Meyer et al. 2004; Kim et al. 2005; Hillenbrand et al. 2008; Carpenter et al. 2009), the A star GTO programs (Rieke et al. 2005; Su et al. 2006), young cluster programs (Gorlova et al. 2006; Siegler et al. 2007), binary star programs (Trilling et al. 2007), as well as their combinations (e.g. Trilling et al. 2008). These observations were done mostly at 24 and $70\,\mu\mathrm{m}$ with the MIPS photometer and resulted in hundreds of detections. At the MIPS sensitivity level, the incidences of debris disks around different-aged stars with spectral classes from A to K are about 15% (Su et al. 2006; Siegler et al. 2007; Trilling et al. 2008; Hillenbrand et al. 2008). The PACS instrument aboard the Herschel Space Observatory is now performing observations (photometry and low-resolution "small maps") at a much higher sensitivity level than that of Spitzer/MIPS. The sub-mm wavelength region is being probed by CSO/SHARC, Herschel/SPIRE, JCMT/SCUBA, APEX/LABOCA, and other instruments. Soon more high-quality data should start coming from JCMT/SCUBA-2 (Matthews et al. 2007).

2.2 Imaging

So far, about 20 of the brightest debris disks have been resolved at various wavelengths from visual through mid- and far-IR to sub-mm and radio; see, e.g., *http://www.circumstellardisks.org*. Scattered light images in the visual and near-IR are being taken, for instance, with HST/ASC and many ground-based instruments in the coronagraphic mode, thermal emission images in the mid-IR with Gemini South/TReCS and KeckII/MIRLIN; the JCMT/SCUBA instrument has been particularly successful in resolving debris disks in the sub-mm. Resolved systems span ages from about 12 Myr for the members of the Beta Pictoris Moving Group (Zuckerman et al. 2001; Ortega et al. 2002) such as β Pic itself (Smith & Terrile 1984) or AU Mic (Kalas et al. 2004) to $\sim$ 4–12 Gyr (Di Folco et al. 2004) for τ Cet (Greaves et al. 2004). All of the disks resolved so far exhibit various structures: rings, inner voids, clumps, spirals, warps, and wing asymmetries. An interpretation of these structures is discussed in Section 7.

2.3 Infrared Spectroscopy

Early successful observations of several debris disks were made with NTT/TIMMI2 (Schütz et al. 2005). However, most of the information comes from the Spitzer/IRS instrument that has taken good-quality spectra of more than a hundred stars from 5 to 35 μm. For instance, Chen et al. (2006) describe IRS spectra of 59 stars with IRAS 60 μm IR excesses, five of which show a clear silicate feature at 10 μm. Often other spectral features are seen that may be indicative of Fe-rich sulfides, water ice, and other compounds (e.g. Lisse et al. 2007). In addition, another Spitzer instrument, MIPS, offered the so-called spectral energy distribution (SED) mode, in which low-resolution spectra in the region from 55 μm to 90 μm have been taken (Chen et al. 2008). In the future, high-quality mid-IR spectra are expected, e.g., from the JWST/MIRI.

2.4 Other Methods

One method is near-IR polarimetry. A certain degree of linear polarization of scattered light coming from the circumstellar debris dust is expected, because it has a flattened, disk geometry (e.g. Krivova et al. 2000). Successful polarimetry observations were done so far only for a few brightest debris disks, such as β Pic (Gledhill et al. 1991; Wolstencroft et al. 1995) and AU Mic (Graham et al. 2007). Such measurements can be particularly useful to further constrain the size distribution and chemical composition of dust (Krivova et al. 2000). Another method is near-IR interferometry, which probes dust in extreme proximity to the stars (the so-called "exozodiacal clouds"). Using this method, a handful of exozodis within 1 AU from the stars was discovered in recent years with the CHARA/FLUOR instrument in the K band at 2.2 μm (Absil et al. 2006; Di Folco et al. 2007; Absil et al. 2008; Akeson et al. 2009) and with the Keck Interferometer Nuller at 10 μm (Stark et al. 2009). An example of more exotic methods suggested to detect debris disks is microlensing (Heng & Keeton 2009).

3 BASIC PHYSICS

Every debris disk is composed of solids, spanning a huge size range from hundreds of kilometers (large planetesimals) down to a fraction of a micrometer (fine dust). These objects orbit the central star and occasionally collide with each other. We start with a brief characterization of their individual orbits and then move on to the mutual collisions.

3.1 Stellar Gravity and Radiation Pressure

The force keeping a planetesimal or a dust grain in a closed orbit is the central star's gravity:

$$\boldsymbol{F}_{\rm g} = -\frac{GM_\star m}{r^3}\boldsymbol{r}, \tag{1}$$

where G is the gravitational constant, $M_\star$ the stellar mass, $\boldsymbol{r}$ the radius vector of the object and m its mass. For the time being, we neglect further possible gravitational forces by planets in the system (see Sect. 7 for a discussion of their effects). At dust sizes ($s \lesssim 1\,{\rm mm}$), the solids are also subject to radiation pressure caused by the central star. Like stellar gravity, radiation pressure scales as the reciprocal of the squared distance to the star, but is directed outward. Thus the two forces can be combined into a "photogravitational" force (Burns et al. 1979) that can be written as

$$\boldsymbol{F}_{\rm pg} = -\frac{GM_\star(1-\beta)m}{r^3}\boldsymbol{r}, \tag{2}$$

where β is the radiation pressure to gravity ratio that depends on the grain size and optical properties. The simplest assumption is that compact grains of spherical shape are characterized by their radius s, bulk density ρ, and radiation pressure efficiency $Q_{\rm pr}$. The last coefficient controls the fraction of the momentum transferred from the infalling radiation to the grain. Its values range from 0 for perfect transmitters to 2 for perfect backscatterers. An ideal absorber's radiation pressure efficiency equals unity. In that case, the β-ratio is given by (Burns et al. 1979)

$$\beta \;=\; 0.574\left(\frac{L_\star}{L_\odot}\right)\left(\frac{M_\odot}{M_\star}\right)\left(\frac{1\,{\rm g\,cm^{-3}}}{\rho}\right)\left(\frac{1\;\mu{\rm m}}{s}\right), \tag{3}$$

where $L_\star/L_\odot$ and $M_\star/M_\odot$ are luminosity and mass of the star in solar units, respectively.

If, by fragmentation or any other erosive process, smaller particles are released from larger ones, they start to "feel" a photogravitational force rather than gravitational force. The smaller the grains, the more the radiation pressure counteracts the central star's gravity. Thus the orbits of small particles differ from those of the parent bodies (Fig. 1 left). A parent body on a circular orbit, for example, releases fragments into bound elliptic orbits with larger semimajor axes and eccentricities up to $\beta = 0.5$. If $0.5 < \beta < 1$, the grain orbits are hyperbolic and thus unbound. For parent bodies in elliptic orbits, the boundaries between bound and unbound orbits are somewhat smeared, because the type of orbit depends on the ejection point. All grains with $\beta < 1$ orbit the star on Keplerian trajectories at velocities reduced by a factor of $\sqrt{1-\beta}$ compared to macroscopic bodies, which are purely under the influence of gravitation. Finally, below the critical size where $\beta = 1$ the effective force is repelling, and the grains move on "anomalous" (i.e., open outward) hyperbolic orbits. Borrowing the terminology from solar system studies (Zook & Berg 1975), we may call dust grains in bound and unbound orbits α-meteoroids and β-meteoroids, respectively.

3.2 Collisions

As the very name "debris disks" suggests, they should incessantly produce "collisional debris," so that destructive collisions must be a dominant process operating in these systems. For collisions to be destructive — and even to occur at sufficient rates – a certain minimum level of relative velocities is necessary. In protoplanetary disks, this condition is not fulfilled, as relative velocities are strongly damped by dense ambient gas, so that the orbits all have low eccentricities and inclinations. In contrast, debris disks are gas-poor, and damping is not efficient at all. However, the absence of damping is necessary, but not sufficient for relative velocities to be high. As a protoplanetary disk transforms to a debris disk in the course of its evolution, solids are expected to preserve a low velocity dispersion they had before the primordial gas removal. Accordingly, to ignite destructive

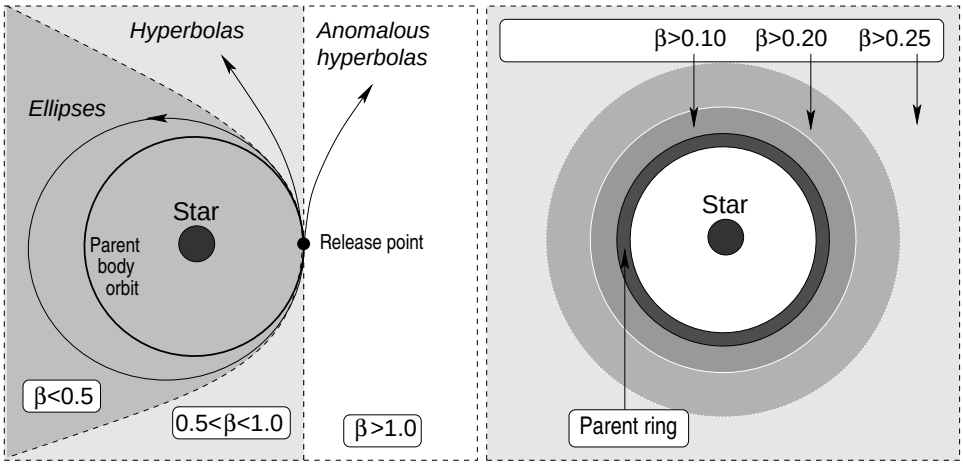

Fig. 1 *Left:* Three possible types of orbits of dust particles under the combined action of stellar gravity and direct radiation pressure. For illustrative purposes, grains are assumed to be released from a circular orbit. *Right:* Schematic of a debris disk produced by a parent planetesimal belt.

collisions, debris disks must be "stirred" by some mechanism (Wyatt 2008). This can be self-stirring by the largest planetesimals (Kenyon & Bromley 2004a) or stirring by planets orbiting in the inner gap of the disk (Wyatt 2005; Mustill & Wyatt 2009). Further possibilities which, however, are not considered typical for the majority of the disks include "fast ignition" by the abrupt injection of a planet (suggestively of Neptune masses) into the disk after planet-planet scattering (Raymond et al. 2009) or external events such as stellar flybys (Kenyon & Bromley 2002).

Once the disk is sufficiently stirred, the collisional cascade sets in. The material is ground all the way down to the dust sizes, until the smallest fragments with $\beta \gtrsim 0.5$ are blown away from the disk by radiation pressure. Note that at dust sizes, stirring is no longer required. As typical eccentricities of grains are of the same order as their β-ratio (e.g. Burns et al. 1979), radiation pressure ensures the impact velocities to be sufficiently high. What is more, some of the hyperbolic grains, β-meteoroids, may be energetic enough to trigger a self-sustained cascade ("dust avalanche") on their way outward through the disk (Artymowicz 1997; Krivov et al. 2000). This process, however, can only be efficient in the dustiest debris disks such as β Pic (Grigorieva et al. 2007).

We now take a more quantitative look at the collisions. An important quantity in the collisional prescription is the critical specific energy for disruption and dispersal, $Q_{\rm D}^{\star}$. It is defined as the impact energy per unit target mass that results in the largest remnant containing half of the original target mass. For small objects, $Q_{\rm D}^{\star}$ is determined solely by the material strength, while for objects larger than ~ 100 m, the gravitational binding energy dominates. As a result, $Q_{\rm D}^{\star}$ is commonly described by the sum of two power laws (see, e.g., Davis et al. 1985; Holsapple 1994; Paolicchi et al. 1996; Durda & Dermott 1997; Durda et al. 1998; Benz & Asphaug 1999; Kenyon & Bromley 2004b; Stewart & Leinhardt 2009):

$$Q_{\rm D}^{\star} = Q_{\rm s} \left(\frac{s}{1\ {\rm m}} \right)^{-b_{\rm s}} + Q_{\rm g} \left(\frac{s}{1\ {\rm km}} \right)^{b_{\rm g}} , \tag{4}$$

where the subscripts s and g stand for the strength and gravity regimes, respectively. The values of $Q_{\rm s}$ and $Q_{\rm g}$ lie in the range $\sim 10^5$–$10^7\,{\rm erg\,g^{-1}}$, $b_{\rm s}$ is between 0 and 0.5, and $b_{\rm g}$ between 1 and 2 (Benz & Asphaug 1999). The critical energy reaches a minimum ($\sim 10^4$–$10^6\,{\rm erg\,g^{-1}}$) at sub-km sizes.

At dust sizes, Equation (4) suggests $\sim 10^8\,\mathrm{erg\,g^{-1}}$, but true values remain unknown, as this size regime has never been probed experimentally. Both colliders are disrupted if their relative velocity $v_{\rm rel}$ exceeds (see, e.g. Krivov et al. 2005, their eq. (5.2))

$$v_{\rm cr} = \sqrt{\frac{2(m_{\rm t}+m_{\rm p})^2}{m_{\rm t}m_{\rm p}} Q^\star_{\rm D}}\,, \tag{5}$$

where $m_{\rm t}$ and $m_{\rm p}$ are masses of the two colliders. Thus two like-sized objects will be destroyed if they collide at a speed exceeding $\sqrt{8Q^\star_{\rm D}}$. For two dust grains, the critical speed is several hundred $\mathrm{m\,s^{-1}}$. At several tens of AU from a star, this would imply eccentricities of ~ 0.1 or higher. Such eccentricities can be naturally attained by dust grains with $\beta \sim 0.1$ as a result of the radiation pressure effect described above.

The actual physics of collisions in debris disks is more complicated. Collisions occur across a size range that is ~ 12 orders of magnitude wide and at quite different velocities. Statistically, collisions between objects of *very* dissimilar sizes (e.g., impacts of dust grains onto "boulders") outnumber those between like-sized objects. Besides, grazing or at least oblique collisions are more frequent than frontal ones. All this leads to a spectrum of possible collisional outcomes that take place simultaneously in the same disk, comprising further growth of large planetesimals, partial destruction (cratering) of one or both projectiles with or without reaccumulation of fragments, as well as a complete disruption of small planetesimals and dust particles. Detailed analyses show that two outcomes are expected to play a crucial role in debris disks: complete disruption and cratering (Thébault & Augereau 2007; Müller et al. 2010).

3.3 Drag Forces

A more accurate, special-relativistic, derivation of the photogravitational force leads to an additional velocity-dependent term that has to be added in the right-hand side of Equation (2) (Burns et al. 1979):

$$\boldsymbol{F}_{\rm PR} = -\frac{GM_\star \beta m}{r^2}\left[\left(\frac{\boldsymbol{vr}}{cr}\right)\frac{\boldsymbol{r}}{r} + \frac{\boldsymbol{v}}{c}\right] \tag{6}$$

with $\boldsymbol{v}$ being the velocity vector of the particle, which is referred to as the Poynting-Robertson (P-R) force. Being dissipative, this force causes a particle to gradually lose its orbital energy and angular momentum. Thus all α-meteoroids move in Keplerian ellipses with reducing semimajor axes a and eccentricities e (Wyatt & Whipple 1950) (except very close to the central star, Breiter & Jackson 1998). On timescales of thousands of years or more the trajectory shrinks to the star.

As stellar electromagnetic radiation gives rise to radiation pressure forces, stellar particulate radiation — stellar wind — causes stellar wind forces. Similarly to the net radiation pressure force, the total stellar wind force can be decomposed to direct stellar wind pressure and stellar wind drag. For most of the stars, the momentum and energy flux carried by the stellar wind is by several orders of magnitude smaller than that carried by stellar photons, so that the direct stellar wind pressure is negligibly small. However, the stellar wind drag forces cannot be ignored, because the stellar wind velocity $v_{\rm sw}$, to replace c in Equation (6), is much smaller than c. Stellar wind forces can be very important in debris disks around late-type stars (Plavchan et al. 2005; Strubbe & Chiang 2006; Augereau & Beust 2006).

Compared to gas-rich protoplanetary disks, debris disks are expected to be extremely gas-poor, because primordial gas disperses on timescales $\lesssim 10\,\mathrm{Myr}$ (Alexander 2008; Hillenbrand 2008). Even so, in the youngest debris disks with ages of 10–30 Myr, little amounts of gas have been detected. Debris disk gas might be either the remnant of the primordial protoplanetary disk or, more likely, of secondary origin. Possible mechanisms for producing secondary gas include photon-induced desorption from solids (Chen et al. 2007) and grain-grain collisions (Czechowski & Mann

2007). Part of the observed gas may also stem from comet evaporation, as inferred from observed time-variable stellar absorption lines (e.g. Ferlet et al. 1987; Beust & Valiron 2007). In some systems, exemplified by β Pic (Olofsson et al. 2001) and HD 32297 (Redfield 2007), evidence for a stable, orbiting gas component was found. Dynamical effects exerted by rotating gas on dust in young debris disks have been studied, for instance, by Thébault & Augereau (2005) and Krivov et al. (2009).

3.4 Other Forces and Effects

Dust grains interacting with the stellar radiation and stellar wind acquire electrostatic charges due to a variety of effects (photoelectron emission, secondary electron emission, sticking of electrons and ions etc.). Under the presence of the star's magnetic field, they experience the Lorentz force. Its influence on the dynamics of interplanetary dust particles in the solar system is well understood. As the dust grains move through the sectored magnetic field of the Sun with alternative polarities, the Lorentz force rapidly changes its direction. The mutual near-cancellation of these contributions is not complete, however. Over long time spans the Lorentz force results in a "Lorentz diffusion," i.e. essentially stochastic changes in a, e and, most importantly, inclination i (Morfill & Grün 1979; Consolmagno 1980; Barge et al. 1982; Wallis & Hassan 1985). The effect becomes significant for grains less than several micrometers in size. The Lorentz force is not included in most of the debris disk models. This is because it affects relatively small grains, which make only a minor contribution to both the total mass budget and the total cross sectional area of the dust disk.

Sublimation, or transition of dust grains from the solid to the vapor state, occurs in the vicinity of the star. The radius of the sublimation zone depends strongly on the material and porosity of the dust grains and on the luminosity of the primary. In the solar system, silicate and carbonaceous grains sublimate at 2–4 solar radii from the Sun (e.g. Kimura et al. 1997; Krivov et al. 1998). However, for a mixture of water ice and organic material, the sublimation distance in the solar system is as large as $\sim 20\,\mathrm{AU}$, and increases to $30 - 40\,\mathrm{AU}$ around luminous A-stars (Kobayashi et al. 2009).

A number of more exotic effects may influence the dust particles themselves and their dynamics (Burns et al. 1979; Kapišinský 1984). Some are related to the fact that the star is not a point-like object (differential Doppler effect, radiation pressure from an extended source). Others stem from stellar radiation together with rotation of objects (Yarkovsky effect, windmill effect, Radzievsky effect). Still others are related to modification of the grain properties by the environment (sputtering by plasma or interstellar grains, packing effect, electrostatic breakup), etc. None of these, however, seem to be of generic importance for debris disks, requiring either closeness to the star, smallness of particles, or special material compositions.

4 MODELS

4.1 Numerical Simulation Methods

As described in Section 3, each debris disk can be treated as an ensemble of objects of different sizes (from dust to planetesimals) that orbit the star under the influence of gravity, radiation pressure, and other forces. In addition, they experience collisions which destroy or erode these objects and produce new ones, called collisional fragments. Such a system can be numerically modeled by a variety of methods (see Krivov et al. 2005, for a summary) that can be classified into three major groups: N-body simulations, statistical approaches, and hybrid methods.

N-body codes follow trajectories of individual disk objects by numerically integrating their equations of motion. During numerical integrations, instantaneous positions and velocities of particles are stored. Assuming that the objects are produced and lost at constant rates, this allows one to calculate a steady-state spatial distribution of particles in the disk. Then, collisional velocities and rates can be computed and collisions can be applied. It is usually assumed that each pair of objects

that come in contact at a sufficiently high relative velocity is eliminated from the system without generating smaller fragments (Lecavelier des Etangs et al. 1996; Stark & Kuchner 2009; Krivov et al. 2009) or produces a certain number of fragments of equal size (Wyatt 2006). The N-body method is able to handle an arbitrarily large array of forces and an arbitrarily complex dynamical behavior of disk solids driven by these forces. Accordingly, it is superior to other methods in characterization of structures in debris disks arising from interactions with planets, ambient gas, or the interstellar medium. However, this method cannot treat a large number of objects sufficient to cover a broad range of particle masses and thus is less successful in modeling the collisional cascade. In particular, an accurate characterization of the size distribution with N-body codes is hardly possible.

Statistical method effectively replaces particles themselves with their distribution in an appropriate phase space. The ideas trace back to the classical calculation of the velocity distribution in particle ensembles with the Boltzmann equation (Boltzmann 1896; Chapman & Cowling 1970) and of the mass (or size) distribution with the coagulation equation (Smoluchowski 1916; Chandrasekhar 1943). Note that the term "coagulation equation" is actually used regardless of whether the colliding particles merge, fragment, or get destroyed. In applications to planetesimal and debris disks, one introduces a mesh of several variables comprising, for instance, mass, distance, and velocity (Spaute et al. 1991; Weidenschilling et al. 1997; Kenyon & Luu 1998, 1999a,b; Kenyon & Bromley 2002, 2004a,c; Thébault et al. 2003; Thébault & Augereau 2007) or mass and orbital elements (Dell'Oro & Paolicchi 1998; Dell'Oro et al. 1998, 2001, 2002; Krivov et al. 2005). The number of particles in each bin of the mesh at successive time instants is computed by solving equations that describe gain and loss of objects by collisions and other physical processes. Many of the results presented in this paper (e.g., Fig. 2) were obtained with the code ACE (Analysis of Collisional Evolution) that simulates the disks in such a manner, using a 3D mesh of masses, pericentric distances, and eccentricities (Krivov et al. 2005, 2006, 2008). Statistical codes are much more accurate in handling collisions than N-body ones, but treat dynamics in a simplified way, for instance, by averaging over angular orbital elements. For this reason, they are less suitable for simulation of structures in debris disks.

Lastly, *hybrid codes* (Weidenschilling et al. 1997; Goldreich et al. 2004) combine N-body integrations of a few large bodies (planets, planetary embryos, biggest planetesimals) with a statistical simulation of numerous small planetesimals and dust. Such codes, originally developed for planetesimal accretion, have also been applied to debris disks (e.g. Bromley & Kenyon 2006; Kenyon & Bromley 2008). Finally, a stand-alone "superparticle" method developed to study major collisional break-ups in debris disks (Grigorieva et al. 2007) should be mentioned. This method, too, combines N-body and statistical approaches, although in a different way.

4.2 A "Standard Model" for a Debris Disk

A standard model of a debris disk can be devised by considering two major effects, stellar photogravity and collisions, and neglecting the drag forces and all other processes (e.g. Thébault et al. 2003; Krivov et al. 2006; Strubbe & Chiang 2006; Thébault & Augereau 2007; Löhne et al. 2008; Krivov et al. 2008; Thébault & Wu 2008). Imagine a relatively narrow belt of planetesimals ("birth ring" or "parent ring") in orbits with moderate eccentricities and inclinations, exemplified by the classical Kuiper belt in the solar system (Fig. 1 right). The planetesimals orbiting in the birth ring undergo collisional cascades that grind the solids down to dust. At the smallest dust sizes, stellar radiation pressure effectively reduces the mass of the central star and quickly (on a dynamical timescale) sends the grains into more eccentric orbits, with their pericenters still residing within the birth ring while the apocenters are located outside the ring. As a result, the dust disk extends outward from the planetesimal belt. The smaller the grains are, the more extended their "partial" disk is. The tiniest dust grains, for which the radiation pressure effectively reduces the physical mass by half, are blown out of the system in hyperbolic orbits. The radiation pressure blowout of the smallest collisional debris represents the main mass loss channel in such a disk.

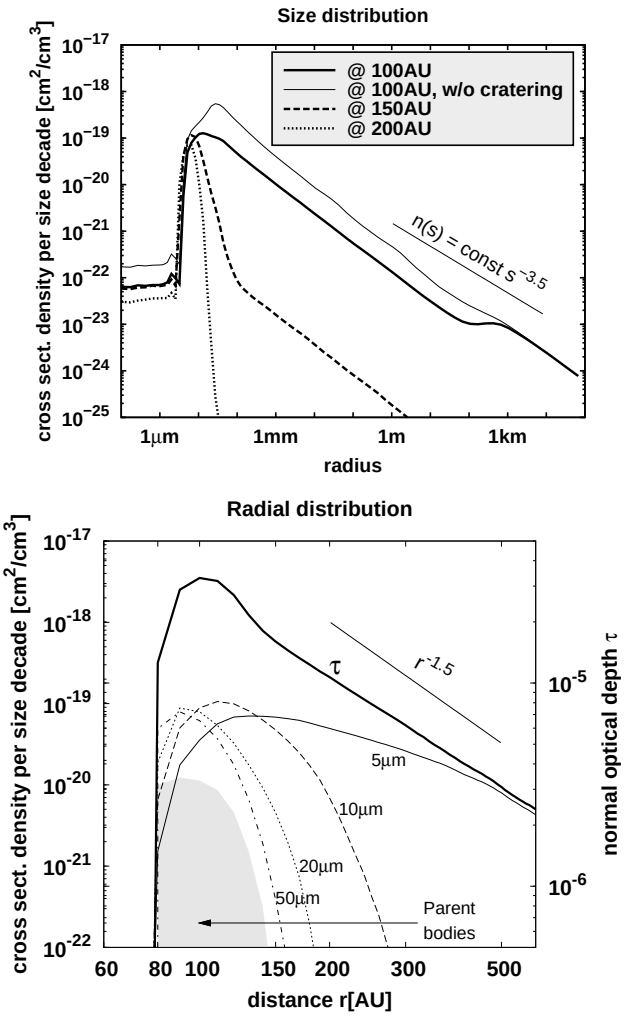

Fig. 2 Modeled dust distributions in a collision-dominated debris disk, here: the "reference" model of Müller et al. (2010). *Upper:* size distribution at different distances from the star with catastrophic and cratering collisions included in the model (*thick lines*). For comparison, a distribution at 100 AU computed without cratering is also shown (*thin solid line*). The straight line depicts the Dohnanyi (1969) distribution for comparison. *Bottom:* radial distribution of different-sized grains (*thin lines*), as well as the overall radial profile of the normal geometrical optical depth (*thick solid line*). The straight line is the $r^{-1.5}$ analytic prediction for the optical depth (Strubbe & Chiang 2006).

One expects a balance between the production of dust by the collisional cascade and its losses by radiation pressure blowout. If such a balance exists, the amounts of particles with different sizes on different orbits stay constant relative to each other, and a debris disk is said to be in a quasi-steady state. However, the absolute amounts should adiabatically decrease with time, because the material at the top-end of the size distribution is not replenished (therefore "quasi"). For brevity, "quasi" is often omitted and a simple "steady state" is used. Basic properties of steady-state disks, derived analytically (e.g. Strubbe & Chiang 2006) and by numerical simulations with statistical

codes (Krivov et al. 2006; Thébault & Augereau 2007) are described in subsequent subsections. The steady-state evolutionary regime can be perturbed, for instance, by occasional collisional break-ups of the largest planetesimals or by "shake-downs" of the system due to instability of nearby planets. After such events, the disk needs some time to relax to a new steady state.

4.3 Collision-Dominated and Transport-Dominated Disks

The model just described is only valid if the collisional timescale is shorter than the characteristic timescale of the drag forces. Such disks are usually referred to as collision-dominated, as opposed to systems that – at dust sizes – are transport-dominated (e.g. Krivov et al. 2000). In the latter case, radial transport of dust material by various drag forces occurs on shorter timescales than collisions. Then, additional removal mechanisms may play a significant role. For example, Poynting-Robertson (P-R) drag can bring grains close to the star where they would sublimate or deliver them into the planetary region where they would be scattered by planets. To be transport-dominated, the system should either have an optical depth below current detection limits (Wyatt 2005) or be subject to transport mechanisms other than P-R drag, such as strong stellar winds around late-type stars (Plavchan et al. 2005; Strubbe & Chiang 2006; Augereau & Beust 2006). Most debris disks detected so far are thought to be collision-dominated. Accordingly, transport-dominated systems will not be considered here.

Note that at sufficiently large sizes, all disks are dominated by collisions. This is because the lifetime against catastrophic collisions in a disk with a size distribution $\propto s^{-3.5}$ discussed below scales $\propto \sqrt{s}$ (see, e.g., Appendix A in Wyatt et al. 1999), whereas any drag force is proportional to the ratio of the mass and cross section, i.e. $\propto s$. For instance, the interplanetary dust cloud in the solar system at $1\,\mathrm{AU}$ from the Sun is tenuous enough to be P-R-dominated at dust sizes, but is collision-dominated above $s \approx 100\,\mu\mathrm{m}$ (Grün et al. 1985).

4.4 Size and Radial Distribution in Collision-Dominated Disks

We now consider the typical size and radial distribution of material in a steady-state collision-dominated debris disk, seen in simulations. As an example, we take the "reference model" of the debris disk of Vega from Müller et al. (2010) that assumes a parent ring between ≈ 80 and $\approx 120\,\mathrm{AU}$. However, the results are generic and qualitatively hold for all collision-dominated disks; Figure 2 (upper) depicts the size distribution. Most noticeable is the peak at the particle size that corresponds to $\beta \sim 0.5$, where the radiation pressure is half as strong as gravity. For the Vega disk, this blowout radius is $s_{\mathrm{blow}} \approx 4\,\mu\mathrm{m}$. Below this size, bound orbits are rare (and below the size where $\beta = 1$ they are impossible), and the grains are blown away on a disk-crossing timescale of the order of 10^2 to 10^3 yr. Typically, the amount of blowout grains instantaneously present in the steady-state system is much less than the amount of slightly larger grains in loosely bound orbits around the star. This is because the production rate of the grains of sizes slightly less and slightly greater than s_{blow} is comparable, but the lifetime of bound grains (due to collisions) is much longer than the lifetime of blowout grains (disk-crossing timescale). This explains a drop in the size distribution around the blowout size seen in the upper panel of Figure 2. The size distribution above s_{blow} sensitively depends on the collisional outcome model assumed, which is seen by comparing the distributions at $100\,\mathrm{AU}$ computed with and without taking cratering collisions into account. The overall size distribution inside the parent ring (the $100\,\mathrm{AU}$ curve) at sizes $s \gg s_{\mathrm{blow}}$ roughly follows the classical Dohnanyi power law, which corresponds to the differential size distribution $n \propto s^{-3.5}$. That law was theoretically derived by Dohnanyi (1969) for a collisional cascade in a system without sources and sinks, composed of objects with $Q_{\mathrm{D}}^{\star} = \mathrm{const}$. The deviations of the size distribution in Figure 2 (upper) from the Dohnanyi law reflect the size dependence of $Q_{\mathrm{D}}^{\star}$, given by Equation (4). A notch at $s \sim 100\,\mathrm{m}$ corresponds to the minimum of $Q_{\mathrm{D}}^{\star}$, and the slope at larger sizes is slightly steeper than

Dohnanyi's, because $Q_{\rm D}^{\star}$ increases with size in the gravity regime (Durda & Dermott 1997). Another generic feature of the size distribution is that it becomes narrower at larger distances from the star. At twice the distance of the parent ring, 200 AU, the distribution transforms to a narrow peak around $\sim 2s_{\rm blow}$ which is only composed of small, high-β, barely bound grains blown by radiation pressure into eccentric orbits with large apocentric distances.

The spatial distribution of dust in the same modeled disk is illustrated by Figure 2 (bottom). As noted above, smaller grains with higher β ratios acquire higher orbital eccentricities. Since the eccentricities of particles slightly above the blowout limit ($s = 5\,\mu$m) are the highest, their radial distribution is the broadest, whereas larger particles stay more confined to their birth regions. In the figure, this effect can be seen from how the curves gradually change from the smallest ($s = 5\,\mu$m) to the largest bound grains ($50\,\mu$m). The latter essentially follow the distribution of their parent bodies. In addition, the same figure shows the radial profile of the normal geometrical optical depth. The slope of $\tau \propto r^{-\alpha}$ is close to $\alpha = 1.5$, as predicted analytically by Strubbe & Chiang (2006) for collision-dominated disks.

4.5 Disk Appearance at Different Wavelengths

Size segregation of dust in debris disks described above means that, in resolved images at different wavelengths, the same disk would look different (Fig. 3). Measurements at longer wavelengths (sub-mm) probe larger grains, because they are cooler (see Sect. 5), and thus trace the parent ring. Such observations may also reveal clumps, if for instance there is a planet just interior to the inner rim of the parent ring, and parent planetesimals and their debris are trapped in external resonances, similar to Plutinos in a 3:2 resonance with Neptune (Wyatt 2006; Krivov et al. 2007). At shorter wavelengths (far-IR, mid-IR), smaller (warmer) grains are probed. Thus the same disk appears much larger. The image may be featureless, even if the parent ring is clumpy, because strong radiation pressure (Wyatt 2006) and non-negligible relative velocities (Krivov et al. 2007) would liberate small particles from resonant clumps. As a result, they would form an extended disk, as described above, regardless of whether their parent bodies are resonant or not. Finally, at the shortest wavelengths of thermal emission, only the hottest closest-in grains are evident in the observations, and thus again only the parent ring is seen.

4.6 Scaling Laws for Evolution of Collision-Dominated Disks

Some useful laws that describe quasi-steady state evolution of collision-dominated disks have been found (Wyatt et al. 2007a; Löhne et al. 2008; Krivov et al. 2008).

1. *Dependence of evolution on initial disk mass.* Consider a narrow parent ring with initial mass $M(t = 0) \equiv M_0$ at distance r from the star with age t. Denote by $F(M_0, r, t)$ any quantity directly proportional to the amount of disk material in any size regime, from dust grains to planetesimals. In other words, F may equally stand for the total disk mass, the mass of dust, its total cross section, etc. There is a scaling rule (Löhne et al. 2008):
$$F(xM_0, r, t) = xF(M_0, r, xt), \tag{7}$$
valid for any factor $x > 0$. This scaling is an *exact* property of every disk of particles, provided these are produced, modified and lost only in binary collisions, rather than in any other physical processes.
2. *Dependence of evolution on distance.* Another scaling rule is the dependence of the evolution timescale on the distance from the star (Wyatt et al. 2007a; Löhne et al. 2008). Then
$$F(M_0, xr, t) \approx F(M_0, r, x^{-4.3}t). \tag{8}$$
Unlike Equation (7), this scaling is approximate.

3. *Dust mass as a function of time.* Finally, the third scaling rule found in Löhne et al. (2008) is the power-law decay of the dust mass

$$F(M_0, r, xt) \approx x^{-\xi} F(M_0, r, t), \tag{9}$$

where $\xi \approx 0.3 \ldots 0.4$. This scaling is also approximate and, unlike Equations (7) and (8), only applies to every quantity directly proportional to the amount of *dust*. In this context, "dust" refers to all objects in the strength rather than the gravity regime, implying radii less than about 100 meters. The scaling is sufficiently accurate for disks, which are much older than the collisional lifetime of these $100\,\mathrm{m}$-sized bodies.

5 DEBRIS DISKS: SEEING DUST

5.1 Dust Temperature and Fractional Luminosity

Observational data for most of the debris disks are pretty scarce and consist only of a few photometric points indicative of the IR excess. In many cases, these points can be fitted with a spectral energy distribution (SED) of a blackbody with a single temperature. Two useful quantities that can be derived from such observations are the dust temperature T_d and the dust fractional luminosity f_d, defined as a ratio of the bolometric luminosities of the dust and the star.

Both T_d and f_d can be estimated from the wavelength where the dust emission flux peaks, $\lambda^\mathrm{d}_\mathrm{max}$, and the maximum flux itself, $F^\mathrm{d}_\mathrm{max}$ (Wyatt 2008). (Henceforth, any "flux" is assumed to be specific flux per unit frequency interval.) If dust behaves as a blackbody, Wien's displacement law gives:

$$T_\mathrm{d} = 5100\,\mathrm{K} \left(\frac{1\,\mu\mathrm{m}}{\lambda^\mathrm{d}_\mathrm{max}} \right). \tag{10}$$

Assuming, further, that the stellar photosphere also emits as a blackbody, it is straightforward to find

$$f_\mathrm{d} = \frac{F^\mathrm{d}_\mathrm{max}}{F^\star_\mathrm{max}} \frac{\lambda^\mathrm{d}_\mathrm{max}}{\lambda^\star_\mathrm{max}}, \tag{11}$$

where $\lambda^\star_\mathrm{max}$ and $F^\star_\mathrm{max}$ are the wavelength where the stellar radiation flux has a maximum and the maximum flux itself, respectively. Note that Equation (11) can only be used for ballpark estimates, because the actual stellar spectrum may deviate from a single blackbody spectrum considerably. A more accurate method to determine f_d that does not imply any blackbody assumptions is using its definition: one calculates the bolometric dust luminosity from the SED, uses the bolometric luminosity of the star from catalogs, and takes their ratio.

5.2 Dust Location, Dust Mass, Dust Sizes

Keeping the assumption that dust interacts with the stellar radiation as a blackbody and making some assumptions about the disk geometry, a number of further useful physical parameters can be derived from T_d and f_d (Wyatt 2008). For instance, assuming the disk to be a narrow ring between $r - \mathrm{d}r$ and $r + \mathrm{d}r$, dust temperature gives the distance from the star:

$$r = \left(\frac{278\,\mathrm{K}}{T_\mathrm{d}} \right)^2 \left(\frac{L_\star}{L_\odot} \right)^{0.5}, \tag{12}$$

whereas f_d is directly related to the total cross-sectional area of dust σ_d,

$$\sigma_\mathrm{d} = 4\pi r^2 f_\mathrm{d}, \tag{13}$$

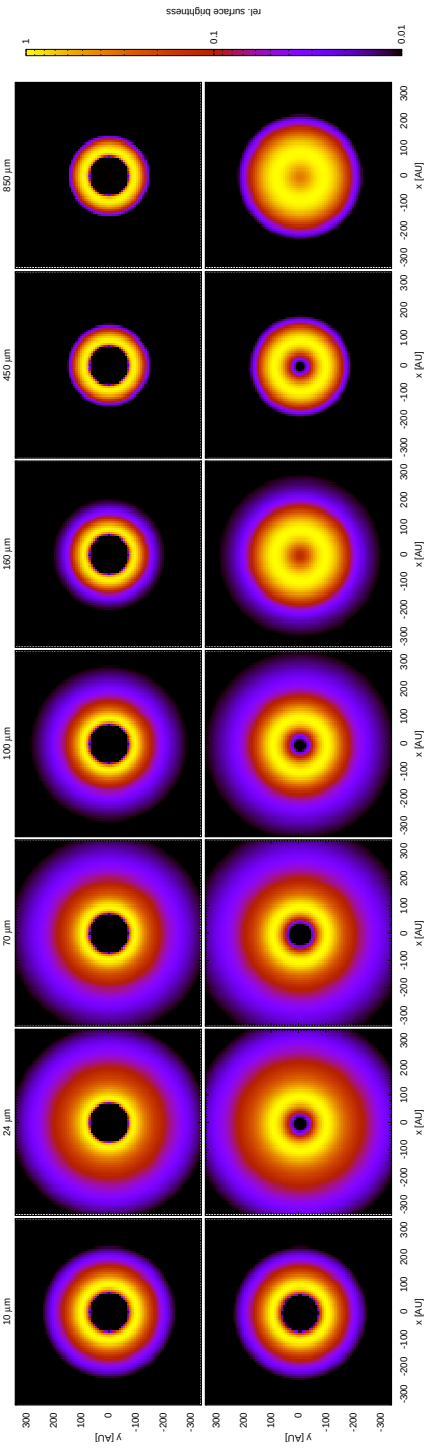

Fig. 3 Appearance of a debris disk at different wavelengths from 10 to 850 μm. *Top row:* synthetic images of the Vega disk, based on the "reference" model of Müller et al. (2010). *Bottom row:* the same images convolved with the Point-Spread Function (PSF), which we assumed to be a Gaussian with widths (σ) of 0.089″ at 10 μm (Keck, mirror diameter 10 m), 2.37″ at 24 μm and 1.77″ at 70 μm (Spitzer/MIPS, 0.9 m), 2.53″ at 100 μm and 4.05″ at 160 μm (Herschel/PACS, 3.5 m), 2.66″ at 450 μm and 5.03″ at 850 μm (JCMT/SCUBA, 15 m). These convolved images show how the Vega disk would appear in observations with the best present-day instruments operating at the respective wavelengths. Note that in actual sub-mm images, the Vega disk appears clumpy (Holland et al. 1998; Marsh et al. 2006), which is not seen here, because the model by Müller et al. (2010) is rotationally-symmetric. *Courtesy: Sebastian Müller.*

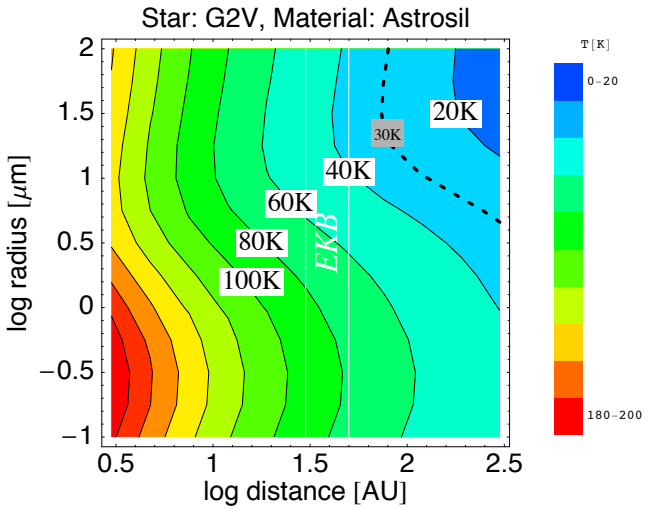

Fig. 4 Calculated temperature of different-sized astrosilicate (Laor & Draine 1993) grains at different distances from a G2V star. *Courtesy: Sebastian Müller.*

and to the normal geometrical optical depth $\tau_\perp$,

$$\tau_\perp = (r/\mathrm{d}r) f_\mathrm{d}. \tag{14}$$

Dust mass M_d can be derived from fractional luminosity as well. However, this estimation requires further assumptions, namely about the dust bulk density ρ_d and a "typical" dust size s_d (which is poorly defined, because f_d-dominating and M_d-dominating sizes are different). Then,

$$M_\mathrm{d} = \frac{16}{3} \pi \rho_\mathrm{d} s_\mathrm{d} r^2 f_\mathrm{d}. \tag{15}$$

More detailed analyses go beyond the assumptions of blackbody, confinement of dust to a narrow radial zone, and like-sized dust grains. A usual procedure (e.g. Wolf & Hillenbrand 2003) is to assume one or another chemical compositions of dust, as well as a radial distribution of dust from r_min to r_max and a size distribution from s_min to s_max. Both distributions are usually postulated to be power laws. Both the limits and slopes of these power laws are treated as free parameters, and their values are sought by fitting the SED and, where available, the resolved images.

This procedure is very efficient, has been implemented in a number of codes (e.g. Wolf & Hillenbrand 2005) and is intensively used in interpretation of the debris disk observations. A short summary of the essential results is given below. However, it reveals two problems that need to be mentioned. One is that relaxing the blackbody assumption makes dust temperature dependent not only on the dust location, but also on the particle sizes (Fig. 4). Roughly speaking, smaller grains at the same distance are warmer than larger ones. This leads to a fundamental degeneracy between distance and size, as the same SED can be produced equally well by a disk of smaller grains farther out from the star and by a disk of larger grains closer in. One way to break this degeneracy is to invoke information from resolved images, if these are available, as they show directly where most of the emitting dust is located. Another method is to invoke theoretical constraints, notably to assume that the minimum grain size s_min is close to the radiation pressure blowout limit s_blow (Sect. 4). Another problem of the fitting approach described above is more difficult to cope with. It is rooted in the assumption that radial and size distribution are both power laws, independent of each other. As

we saw, this is not what is expected from the debris disk physics. Instead, one expects the size distribution to strongly depend on distance and conversely, the radial distribution to be very dissimilar for grains of different sizes. Additionally, both size and radial distribution can substantially depart from single power laws (Fig. 2).

5.3 Outer Disks, Inner disks, and Exozodiacal Clouds

We now come to a brief overview of essential results on dust location and masses obtained with the procedures described above. For many of the systems, the SED is consistent with a single, radially narrow dust disk. The typical dust temperatures are on the orders of several tens of Kelvin, which correspond to the dust disks located at several tens to a hundred AU from the star. We will refer to them as "outer disks." Such distances readily suggest that the outer disks are likely produced by the Edgeworth-Kuiper belt (EKB) analogs around those stars. However, the typical fractional luminosities of $\sim 10^{-5}$—10^{-3} are at least by two (Vitense et al. 2010) to four (Booth et al. 2009) orders of magnitude more than the fractional luminosity of the presumed EKB dust in the present-day solar system. The derived dust masses in debris disks (up to $s \sim 1\,\mathrm{mm}$, best estimated from sub-mm measurements) are in the range 10^{-3}–10^{0} Earth mass (e.g. Sheret et al. 2004; Williams et al. 2004; Najita & Williams 2005).

There are also systems that cannot be explained with a single outer dust disk. Apart from, or instead of, the cold dust disks, some stars have dust within $\sim 10\,\mathrm{AU}$. The majority of such "inner disks" may be associated with collisionally-evolving asteroid-like belts or sustained by cometary activity (both mechanisms are known to be sources of the zodiacal cloud in the solar system). Alternatively, the fact that many solar-type (FGK) stars show a considerable warm excess at ages $\lesssim 100\,\mathrm{Myr}$, which is about the timescale for accretion of the Earth in the solar system, suggests that inner dust may be debris from terrestrial planet formation (Kenyon & Bromley 2004b). The dust masses in the inner debris disks are estimated to be typically in the range 10^{-8}–10^{-6} Earth mass (e.g. Krivov et al. 2008, and references therein).

Yet closer-in to the central stars, within $1\,\mathrm{AU}$, "exozodiacal clouds" have been detected with near-IR interferometry. The most prominent examples of stars hosting exozodis are Vega (Absil et al. 2006), τ Cet and Fomalhaut (Di Folco et al. 2007; Absil et al. 2008; Akeson et al. 2009), as well as η Crv (Bryden et al. 2009b). The archetypical exozodiacal cloud of Vega has an estimated dust mass of $\sim 10^{-7}$ Earth mass (equivalent to the mass of an asteroid about $70\,\mathrm{km}$ in diameter) and a fractional luminosity of 5×10^{-4}.

5.4 Frequencies of Disks around Stars with Different Spectral Types and Ages

In recent years, detailed statistical studies have been published that show how the parameters of outer and inner dust disks depend on the spectral type of the star as well as on the system's age (Meyer et al. 2004; Beichman et al. 2005; Kim et al. 2005; Rieke et al. 2005; Bryden et al. 2006; Beichman et al. 2006; Su et al. 2006; Gautier et al. 2007; Siegler et al. 2007; Hillenbrand et al. 2008; Meyer et al. 2008; Trilling et al. 2008; Bryden et al. 2009a; Carpenter et al. 2009; Plavchan et al. 2009). These statistics are largely based on the Spitzer/MIPS measurements at 24 and $70\,\mu\mathrm{m}$. Note that for A-type stars, outer EKB-like disks are essentially probed at both wavelengths. However, for G-stars, only $70\,\mu\mathrm{m}$ excesses correspond to the EKB region while $24\,\mu\mathrm{m}$ measurements detect inner dust inside $\sim 10\,\mathrm{AU}$ (see, e.g., fig. 1 in Wyatt 2008). Still longer wavelengths may be required to detect outer disks around K and especially M dwarfs, because EKB-sized disks around such stars are very cold.

About 33% of A-stars over all ages show excess emission at $24\,\mu\mathrm{m}$ and/or $70\,\mu\mathrm{m}$, indicative of outer disks (Su et al. 2006). The disk frequency around A-stars is as high as 60% at $\sim 10\,\mathrm{Myr}$ and

declines to about 10% at 600 Myr (Siegler et al. 2007). In addition, disks around younger stars are brighter, with a possible broad peak of the 24 μm luminosity at $\sim$ 10 Myr (Hernández et al. 2006).

For solar-type (F0–K0) stars, the average frequency of outer disk detections at 70 μm was found to be $\approx$ 16% (Beichman et al. 2006; Bryden et al. 2006; Trilling et al. 2008). For stars cooler than K1, the fraction may drop to 0%–4% (Beichman et al. 2006), and low detection frequencies for K and M stars have been confirmed by other analyses (Gautier et al. 2007; Plavchan et al. 2009). However, as noted above, their detection should be more efficient at wavelengths longer than 70 μm. Indeed, a sub-mm JCMT/SCUBA survey for M dwarfs suggests that the proportion of debris disks is likely higher than that found with Spitzer (Lestrade et al. 2006). The frequencies of disks around FGK stars decline with age more slowly than those of A-type stars. The excess strength, or fractional luminosity, exhibits a smooth decay with the stellar age as well.

All authors point out a decay of the observed mid- and far-IR excesses with the system age. However, the dust fractional luminosity exhibits a large dispersion at any given age even within a narrow range of spectral classes. We will come to the interpretation of the long-term decay in debris disks in Section 6. Apart from the time evolution of the fractional luminosity, attempts have been made to find correlations between the disk radius on age. From IRAS 60 and 100 μm data, Rhee et al. (2007) found that the radii of the largest disks increase with the age, but similar analyses based on 24 and 70 μm Spitzer detections do not reveal any significant correlation (Wyatt et al. 2007b and T. Löhne, pers. comm).

Inner disks with a moderate fractional luminosity around A-type stars are difficult to detect because it requires measurements shorter than 24 μm where the photosphere is bright. Nevertheless, they can be detected through measurements at 24 μm around solar-type stars. The incidences of inner disks drop from 20%–40% at $\sim$ 20 Myr to only a few percent at $\gtrsim$ 1 Gyr (Siegler et al. 2007; Meyer et al. 2008; Carpenter et al. 2009). The detection fraction averaged over the ages is $\approx$ 4% (Trilling et al. 2008). Many older ($\gtrsim$ 100 Myr) FGK stars with inner dust have an abnormally high fractional luminosity, as discussed in Section 6. Apart from the mid-IR photometry, evidence for inner dust can also be found in the Spitzer/IRS spectra in the $\approx$ 5 to 35 μm range. Lawler et al. (2009) analyzed IRS observations of nearby solar-type stars and found an excess of around 12% of them in the long-wavelength IRS band (30–34 μm), but only 1% of the stars have detectable excess in the short wavelength band (8.5–12 μm).

Exozodiacal clouds have been found around at least 20% of AFGKM nearby stars searched with IR interferometry (CHARA/FLUOR and Keck/KIN) (Absil et al., in prep.), There appears to be a weak positive correlation between the incidences of outer disks and exozodis (O. Absil, pers. comm).

5.5 Chemical Composition of Dust

Mid- and far-IR spectra of some debris disks reveal distinctive features (Jura et al. 2004; Chen et al. 2006; Lawler et al. 2009), which allows one to get insight into the mineralogy of the dust grains. For example, spectra of several disks were matched by a mixture of amorphous and crystalline silicates, silica, and several other species (Schütz et al. 2005; Beichman et al. 2005; Lisse et al. 2007; Lisse et al. 2008; Lisse et al. 2009), including possibly water ice (Chen et al. 2008). The most detailed study was performed for the systems HD 69830 (Beichman et al. 2005; Lisse et al. 2007), HD 113766 (Lisse et al. 2008), and HD 172555 (Lisse et al. 2009). However, interpretation of spectra is difficult and involves degeneracies, since the same spectra can be fitted with different mixtures of materials. Furthermore, laboratory spectra of various samples used as a reference have been obtained under conditions (grain sizes and temperature) that do not necessarily match those in real disks. Furthermore, the laboratory spectra can differ from one measurement technique to another (e.g., KBr pellets vs. free-floating particles, see Tamanai et al. 2006). Despite these caveats, the results are useful. Besides the chemical composition, some constraints can be placed on dust grain

sizes and morphology. For instance, the very presence of distinctive spectral features is indicative of small grains.

6 DEBRIS DISKS: THINKING OF PLANETESIMALS

6.1 Modeling "from the Sources"

Results outlined in the previous section describe the "visible" dust component in debris disks, but they do not directly describe the dust parent bodies and dust production mechanisms. Therefore, many of the basic parameters of the debris disk remain obscure. For instance, while the cross-sectional area of the disk and thus the observed luminosity are dominated by small particles at dust sizes, the bulk of a debris disk's mass is hidden in invisible parent bodies and cannot be directly constrained from analysis of the dust emission. Equally, it remains unknown where exactly the planetesimals are located, although one expects that they orbit the star roughly where most of the dust is seen. Many properties of the planetesimals, such as their dynamical excitation, size distribution, mechanical strength, and porosity, etc., remain completely unclear.

There is no direct way to infer the properties of invisible planetesimal populations from the observed dust emission. Dust and planetesimals can only be linked through models. This is done in two steps. First, collisional models can be used to predict, for a given planetesimal family (mass, location, age, etc.), the distribution of dust. Such models, both analytical and in the form of numerical codes, have become available in recent years (e.g. Thébault et al. 2003; Krivov et al. 2006; Thébault & Augereau 2007; Wyatt et al. 2007a; Löhne et al. 2008). After that, thermal emission models, described in Section 5, have to be employed to compute the resulting dust emission. Comparison of that emission to the one actually observed would then reveal probable properties of the dust-producing planetesimal families.

6.2 Constraints from Statistics of Debris Disks

One way to constrain planetesimal properties with this method is to develop models for a long-term evolution of disks and to compare their predictions with the statistics of debris disks of different ages. As noted above, there is a general tendency of disk dustiness to decay with time, and this is attributed to the collisional depletion of planetesimal families. In an attempt to gain theoretical understanding of the observed evolution, Dominik & Decin (2003) assumed that dust is produced in collisions among equally-sized "comets." If this dust is removed by collisions, the steady-state amount of dust in such a system is proportional to the number of comets. This results in an $M/M_0 \approx \tau/t$ dependence for the amount of dust and for the number of comets or the total mass of the disk. Under the assumption of a steady state, this result is valid even for more complex systems with continuous size distributions from planetesimals to dust. Tenuous disks, where the lifetime of dust grains is not limited by collisions but by transport processes like the Poynting-Robertson drag (Artymowicz 1997; Krivov et al. 2000; Wyatt 2005), should follow $M \propto t^{-2}$ rather than $M \propto t^{-1}$. However, slopes as steep as $M \propto t^{-2}$ are not consistent with observations. Assuming a power-law dependence $t^{-\xi}$, Greaves & Wyatt (2003) reported $\xi \lesssim 0.5$, Liu et al. (2004) gave $0.5 < \xi < 1.0$, and Greaves (2005) and Moór et al. (2006) derived $\xi \approx 1.0$. Fits of the upper envelope of the distribution of luminosities over the age yielded $\xi \approx 1.0$ as well (Rieke et al. 2005). This is an indication that the observed cold debris disks are collision-dominated.

Wyatt et al. (2007a) lifted the most severe simplifying assumption of the Dominik-Decin model, that of equal-sized parent bodies. A debris disk they consider is no longer a two-component system consisting of "comets + dust." Instead, it is a population of solids with a continuous size distribution, from planetesimals down to dust. A key parameter of the description by Dominik & Decin (2003) is the collisional lifetime of comets, τ. Wyatt et al. (2007a) replaced it with the lifetime of the largest planetesimals and worked out the dependencies on this parameter in great detail. Since the

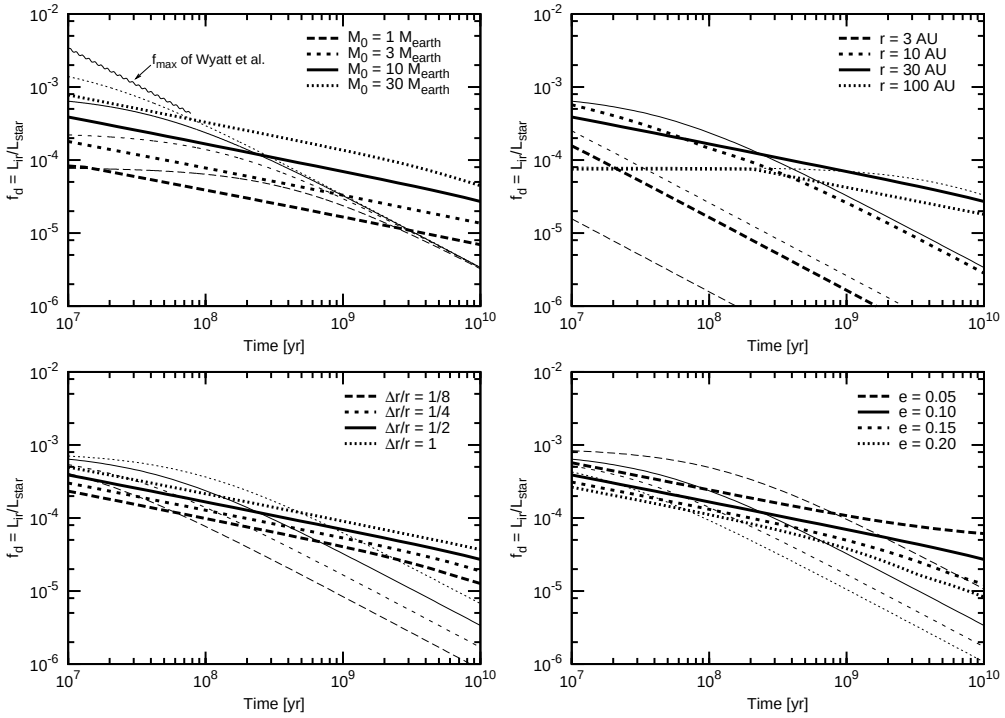

Fig. 5 Fractional luminosity of dust around a solar-like star as a function of age. Thick lines: analytic model of Löhne et al. (2008); thin lines: Eq. (20) of Wyatt et al. (2007a) with $Q_{\rm D}^* = 3 \times 10^4\,{\rm erg\,g^{-1}}$ (constant in their model), $D_{\rm c} = 60\,{\rm km}$. Different panels demonstrate dependence on different parameters: $M_{\rm disk}$ *(top left)*, r *(top right)*, ${\rm d}r/r$ *(bottom left)*, and e *(bottom right)*. A standard case with $M_* = L_* = 1$, $M_{\rm disk} = 10 M_\oplus$, $r = 30$ AU, ${\rm d}r/r = 1/2$, and $e = 0.10$ is shown with solid lines in all panels. *Adapted from Löhne et al.* (2008).

collisional timescale is inversely proportional to the amount of material, $\tau \propto 1/M_0$, the asymptotic disk mass becomes independent of its initial mass (Fig. 5, top left). Only dynamical quantities, i.e. the disk's radial position and extent, the orbiting objects' eccentricities and inclinations, and material properties, i.e. the critical specific energy and the disruption threshold, as well as the type of the central star, determine the very-long-term evolution (Fig. 5, thin lines).

Most recently, Löhne et al. (2008) lifted a major assumption in Wyatt et al. (2007a) that the critical specific energy needed for disruption is constant across the full range of sizes, from dust to the largest planetesimals. As a result, the size distribution of material is no longer a single power law. One consequence is that at actual ages of debris disks between ∼10 Myr and ∼10 Gyr, the decay of the dust mass and the total disk mass follows different laws. The reason is that, in all conceivable debris disks, the largest planetesimals have longer collisional lifetimes than the system's age, and therefore did not have enough time to reach collisional equilibrium. The mass of visible dust at any instant of time is determined by planetesimals of intermediate size, whose collisional lifetime is comparable with the current age of the system, with that "transitional" size gradually increasing with time. Under standard assumptions, the dust mass, fractional luminosity, and thermal fluxes all decrease as $t^{-\xi}$ with $\xi = 0.3 \ldots 0.4$ (cf. Eq. (9)). However, specific decay laws of the total disk mass and the dust mass, including the value of ξ, largely depend on planetesimal properties, such as the

critical fragmentation energy as a function of size, the "primordial" size distribution of the largest planetesimals, as well as the characteristic eccentricity and inclination of their orbits.

6.3 Systems with Abnormally High Fractional Luminosity

Both Wyatt et al. (2007a) and Löhne et al. (2008) models reproduce the observed statistics of "cold" and many "warm" debris disks obtained with the Spitzer/MIPS instrument reasonably well. However, there are individual systems that are not consistent with the models. One implication of the above models is that they predict a certain maximum fractional luminosity $f_{\max}$ for a given age that could be produced by a debris disk collisionally evolving in a steady-state regime. Assuming physically reasonable initial disk masses of $\lesssim 30 M_{\oplus}$ (corresponding to the mass of solids in the minimum-mass solar nebula), $f_{\max}$ of debris disks around solar-type stars older than $\sim 1\,\mathrm{Gyr}$ would be as low as $\sim 10^{-4}$ (Fig. 5, top left). However, some known debris disks have $f \gg f_{\max}$. These are "warm" disks within $\sim 10\,\mathrm{AU}$, exemplified by the debris disk of an A star ζ Lep (Moerchen et al. 2007), as well as some disks of FGK stars: HD 23514 (Rhee et al. 2008), η Crv (Wyatt et al. 2005), and HD 69830 (Beichman et al. 2005; Lisse et al. 2007; Payne et al. 2009). The same problem arises for exozodiacal clouds, where $f_{\max}$ is quite low because the collisional evolution as close as at $\sim 1\,\mathrm{AU}$ from the star must be very rapid. Thus it is not a surprise that for instance, the exozodi of Vega (Absil et al. 2006) appears "too dusty" to be explained with a steady-state collisional cascade in an asteroid belt analog. The origin of the excessive warm dust and exozodis is currently a matter of debate (Wyatt et al. 2007a; Wyatt 2008; Payne et al. 2009; Wyatt et al. 2010). The observed dust may be debris from recent collisions between two large planetesimals or planetary embryos (Rhee et al. 2008). Alternatively, it can be transported inward from the outer Kuiper belt through one or another mechanism (Wyatt et al. 2007a). It is possible that some of the systems with a high amount of warm dust currently undergo a short-lasting, LHB-like instability phase (Wyatt et al. 2007a; Booth et al. 2009). Finally, systems like η Crv may formally be explained with a collisional cascade in a planetesimal swarm with extremely eccentric orbits ($e \sim 0.99$), although the origin of such a population remains challenging (Wyatt et al. 2010).

6.4 Probing Planetesimal Formation Mechanisms

Since the formation of debris disks is a natural by-product of planetesimal and planet accumulation processes, debris disks can help in distinguishing between possible planetesimal formation mechanisms. The classical scenario is based on a more or less continuous growth of objects from micron-sized grains through bigger aggregates that decouple from the gas to, potentially, planetary embryos. In particular, the last stage has been studied to predict planetesimal distributions (e.g. Kenyon & Bromley 2008, and previous work). However, theoretical considerations have revealed obstacles such as the so-called meter barrier. The latter is a "double bottle-neck" of the growth: first, meter-sized objects should be lost to the central star as a result of gas drag (Weidenschilling 1977; Brauer et al. 2007), and second, further agglomeration of meter-sized objects upon collision is problematic (Blum & Wurm 2008). So, in the last years, a competing scenario was invoked that circumvents these barriers and forms large planetesimals directly through local gravitational instability of solids in turbulent gas disks, which can be triggered, for instance, by transient zones of high pressure (Johansen et al. 2006) or by streaming instabilities (Johansen et al. 2007). Both scenarios result in distinctly different initial conditions for debris disk evolution: the former predicts a substantial population of smaller km-sized planetesimals, while the latter leads to a top-heavy size distribution dominated by objects of roughly 100 km in size. As both scenarios would result in different dustiness of a debris disk at a given age, there appears to be a principal possibility to distinguish between them by confronting the model predictions with debris disk observations (Löhne et al. in prep.).

Constraining the top end of the planetesimal size distribution is also important to understand the mechanism that stirs debris disks. Extending the formalism of Wyatt et al. (2007a,b), Kennedy & Wyatt (2009) devised an analytic model for stirring of debris disks by the formation of Pluto-sized objects. They showed that the 24 and $70\,\mu\mathrm{m}$ statistics of disks around A-type stars is consistent with this self-stirring scenario. That also demonstrated that, to satisfy the constraints from observations such as the early "rise and fall" of peak $24\,\mu\mathrm{m}$ excesses around $\sim 10\,\mathrm{Myr}$ (Sect. 5), the planetesimal belts must be reasonably narrow ($\mathrm{d}r/r \sim 0.5$) and have a minimum radius of $\sim 15\,\mathrm{AU}$.

6.5 Constraints from Debris Disks with Known SEDs

As we could see, useful constraints on the planetesimal properties can be placed for the statistics of many debris disks, even though observational data on each of them can be limited to a few photometric points, such as 24 and $70\,\mu\mathrm{m}$ Spitzer/MIPS measurements. For a limited number of disks, for which photometry points sufficiently probe the entire SED from mid-IR to sub-mm or mm wavelengths, additional constraints can be placed. Krivov et al. (2008) analyzed five G2V stars with good data (IRAS, ISO/ISOPHOT, Spitzer/IRAC, /IRS, /MIPS, Keck II/LWS, and JCMT/SCUBA). For all the five systems, the data points could be reproduced within the error bars with a linear combination of two planetesimal belts (an "asteroid belt" at several AU and an outer "Kuiper belt"). This automatically gave the desired estimates of planetesimals (location, total mass etc.). In particular, the cold emission (with a maximum at the far-IR) is compatible with "large Kuiper belts," with masses in the range 3–50 Earth masses and radii of 100–$200\,\mathrm{AU}$. These large sizes trace back to the facts that the collisional model predicts the observed emission to stem from micron-sized dust grains, whose temperatures are well in excess of a blackbody temperature at a given distance from the star (as discussed, e.g., in Hillenbrand et al. 2008, see also Fig. 4). This conclusion is rather robust against variation in parameters of collisional and thermal emission models, and is roughly consistent with disk radii revealed in scattered light images (e.g. HD 107146, Ardila et al. 2004). Still, quantitative conclusions about the mass and location of the planetesimal belts would significantly depend on (i) the adopted model of collision outcomes (which, in turn, depend on the dynamical excitation of the belts, i.e. on orbital eccentricities and inclinations of planetesimals) and (ii) the assumed grains' absorption and emission efficiencies. For example, a less efficient cratering (retaining more grains with radii $\sim 10\,\mu\mathrm{m}$ in the disk, see Fig. 2 upper) and/or more "transparent" materials (making dust grains of the same sizes at the same locations colder) would result in "shifting" the parent belts closer to the star.

6.6 Constraints from Resolved Debris Disks

The best constraints of planetesimals and their collisional evolution can be found from a combined analysis of the SED and resolved images. Most recently, Müller et al. (2010) analyzed the archetypical debris disk of Vega. It has been argued before that the resulting photometric data and images may be in contradiction with a standard, steady-state collisional scenario of the disk evolution (Su et al. 2005). However, Müller et al. (2010) were able to reproduce the spectral energy distribution in the entire wavelength range from the near-IR to millimeter, as well as the mid-IR and sub-mm radial brightness profiles of the Vega disk with this scenario (Fig. 6). Thus their results suggest that the Vega disk observations are not in contradiction with a steady-state collisional dust production, and they put important constraints on the disk parameters and physical processes that sustain it. The total disk mass in $\lesssim 100$ km-sized bodies is estimated to be ~ 10 Earth masses. Provided that a collisional cascade has been operating over much of the Vega age of ~ 350 Myr, the disk must have lost a few Earth masses of solids during that time. It has also been demonstrated that using an intermediate luminosity of the star between the pole and the equator, as derived from its fast rota-

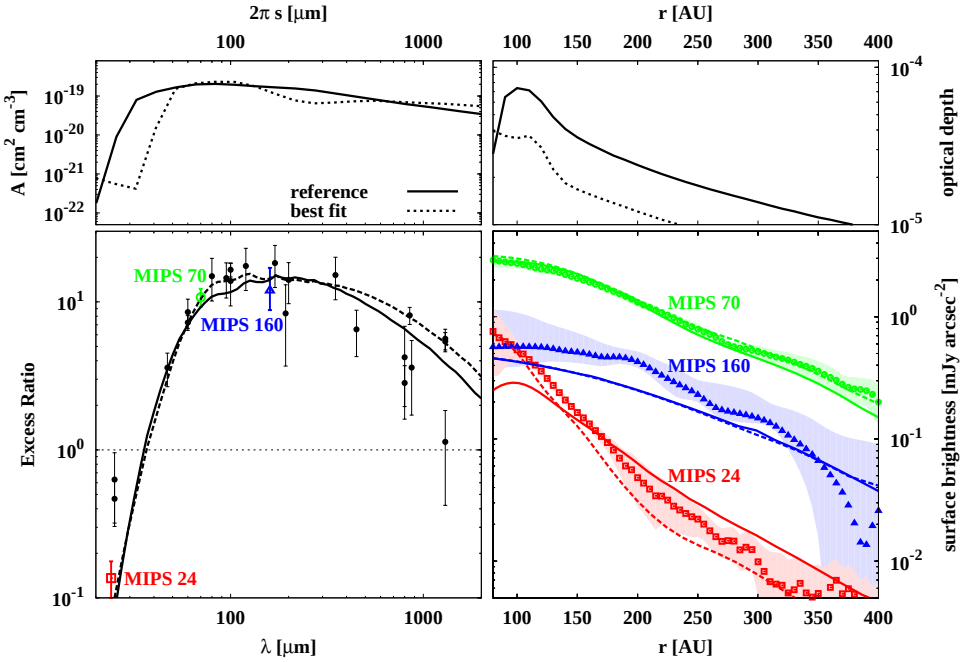

Fig. 6 Two models of the Vega disk (Müller et al. 2010) and their comparison with observations. The "reference model" assumes $L_\star = 28 L_\odot$ and a ring of planetesimals with semimajor axes from 80 to 120 AU and maximum eccentricities of 0.1. The "best-fit model" adopts $L_\star = 45 L_\odot$, a planetesimal ring from 62 to 120 AU with maximum eccentricities of 0.05, and a slightly steeper distribution of fragments in binary collisions. The reason to vary the stellar luminosity is that Vega is a fast rotator (Peterson et al. 2006; Aufdenberg et al. 2006), which makes stellar parameters functions of the stellar latitude. *Top left:* grain size dust distribution (cross sectional area density per size decade) in the "reference model" (*thick solid line*) and the "best-fit model (*dashed line*), both in the center of the initial planetesimal ring. Note our using $2\pi s$ instead of s: since particles with the size parameter $2\pi s/\lambda \sim 1$ emit most efficiently, $2\pi s$ roughly gives the typical wavelength of the emission. This alleviates comparison between the size distribution and the SED (*bottom left*). *Top right*: radial profile of the normal optical depth for the same disk models. *Bottom left*: corresponding SED in the form of the excess ratio (ratio of dust flux to photospheric flux). Symbols with error bars are data points (*large square, large circle, and large triangle* mark 24 μm, 70 μm, and 160 μm excess ratios deduced from Spitzer/MIPS images, respectively). *Bottom right*: modeled (*lines*) and observed (*symbols*, same as in the bottom left panel) surface brightness profiles at 24, 70, and 160 μm. The shaded areas around the data points correspond to their error bars. *Adapted from Müller et al.* (2010).

tion, is required to reproduce the debris disk observations. Finally, it has been shown that including cratering collisions into the model is mandatory.

The appearance of the Vega disk in resolved images, with a ring of large particles seen in sub-mm and an extended sheet of small grains observed in the far- and mid-IR, conforms to the standard debris disk model described in Section 4. Some other resolved disks, such as that of HR8799 (Su et al. 2009), look similar. However, the disks of two other A-type stars, Fomalhaut (Stapelfeldt et al. 2004) and β Leo (Stock et al. in prep.), appear narrow at Spitzer/MIPS wavelengths. The existence of two types of disks – wide ones with fuzzy sensitivity-limited outer edges and narrow ones with well-defined outer boundaries – was also concluded by Kalas et al. (2006) from scattered-

light images. Thébault & Wu (2008) showed that disks with sharp outer edges may arise from a parent belt of planetesimals with very low eccentricities ($e \sim 0.01$ or less). However, this would imply the absence of planetesimals larger than several tens of meters, as these would stir the parent belt to higher eccentricity values. It is challenging to explain why, for instance, the protoplanetary disk of Fomalhaut had built at least one massive planet at $\sim 100\,\mathrm{AU}$ (Kalas et al. 2008), but failed to produce at least kilometer-sized planetesimals only slightly farther out from the star.

7 DEBRIS DISKS: THINKING OF PLANETS

7.1 Structures of Debris Disks as Indicators of Planets

The usefulness of debris disks goes beyond probing the history of planetesimal formation and planetesimal properties: they can also point to planets. Indeed, debris disks gravitationally interact with – often suspected, but as yet undetected – planets at every moment in their life, and various footprints of those interactions can be evident in observations of debris dust. As mentioned above, planets may stir planetesimal disks, launching the collisional cascade. Stirring by planets may be comparable in efficiency with stirring by the largest embedded planetesimals of roughly Pluto's size. Even close-in planets can sufficiently stir the outer disk, if their orbits are eccentric and the systems are sufficiently old (Wyatt 2005; Mustill & Wyatt 2009). For instance, the known radial velocity planet of ϵ Eridani could have ignited its "cold" debris disk (Mustill & Wyatt 2009).

Besides the stirring, a variety of more direct "fingerprints" of planets can exist in the disks. Inner gaps tens of AU in radius which are commonly observed in resolved debris disk images (e.g. Moro-Martín et al. 2007, and references therein) and inferred from the debris disk statistics (Kennedy & Wyatt 2009) are likely the result of clearance by planets (Faber & Quillen 2007) (although they may alternatively be ascribed to preferential planetesimal formation at larger distances in some scenarios, Rice et al. 2006). Accordingly, dedicated quests of planets in systems with known "punched" debris disks by using direct imaging from space or with adaptive optics have been initiated in recent years (Apai et al. 2008). The direct imaging method is technically challenging, and only has chances for success in relatively young systems with ages younger than a few hundred Myr, where the planets have not yet cooled down, but even in that case current searches are not yet sensitive to planets below about one Jupiter mass. Despite that, first planets in the inner voids have recently been found around Fomalhaut (Kalas et al. 2008) and HR 8799 (Marois et al. 2008).

Another indication for planets could be a clumpy disk structure observed, for instance, around Vega (Wyatt 2003) and ϵ Eri (Quillen & Thorndike 2002). Clumps may arise from planetesimal capture into mean motion resonances with unseen planets (e.g. Wyatt 2006; Krivov et al. 2007) or, in systems with a strong P-R or stellar wind drag, from capture of dust grains drifting inward into such resonances (e.g. Liou & Zook 1999; Moro-Martín & Malhotra 2002). A caveat is that individual breakups of large planetesimals could sometimes provide an alternative explanation (Grigorieva et al. 2007). Attempts to find planets in the systems of Vega and ϵ Eri by direct imaging have not yet been successful (Itoh et al. 2006; Marengo et al. 2006; Janson et al. 2007, 2008).

Warps, such as those observed in the β Pic disk, could be due to secular perturbations by a planet in an inclined orbit (Mouillet et al. 1997; Augereau et al. 2001). In fact, there are many more phenomena in the β Pic disk that all point to at least one Jupiter-mass planet at $\sim 10\,\mathrm{AU}$ (see Freistetter et al. 2007, for a summary). The predicted β Pic planet may have already been detected with VLT/NACO by Lagrange et al. (2009), although this result still remains to be confirmed with a second-epoch detection (Fitzgerald et al. 2009). However, large-scale asymmetries observed in resolved debris disks, especially the wing asymmetries in the disks of β Pic (Mouillet et al. 1997), HD 32297 (Kalas 2005; Fitzgerald et al. 2007), and HD 15115 ("the blue needle," Kalas et al. 2007) can be attributed to the disk interaction with the ambient interstellar dust (Artymowicz & Clampin 1997) or gas (Debes et al. 2009).

7.2 Incidences of Debris Disks and Planets around the Same Stars

Current observational statistics shows that at least 7% of stars searched with the radial velocity (RV) method have planets ranging from super-Jupiters down to super-Earths (Udry & Santos 2007)[1]. On the other hand, IR excesses over the photospheric flux indicative of (cold) debris disks have been found for about 15% of main-sequence (MS) stars with spectral classes from A to K (Su et al. 2006; Siegler et al. 2007; Trilling et al. 2008; Hillenbrand et al. 2008). Greaves et al. (2004) were apparently the first to raise natural questions: "do stars with planets also have disks?" and conversely, "do stars with disks also have planets?". Answering these questions is hampered by the fact that the incidences of both planets and disks, retrieved from observational surveys, are biased in various ways, and depend on the current precision or sensitivity of instruments used, and thus may not reflect the reality. It is not a surprise, therefore, that the statistical interrelation between the presence of planets and cold disks remains controversial (Greaves et al. 2004; Beichman et al. 2005; Moro-Martín et al. 2007a; Greaves et al. 2006; Beichman et al. 2006; Kóspál et al. 2009; Bryden et al. 2009a). Nevertheless, it has been found that the incidences of debris disks do not correlate with the stellar metallicity (Greaves et al. 2006; Beichman et al. 2005; Bryden et al. 2009a), whereas the typical metallicity of stars with known planets is well known to be greater than solar (e.g. Wright et al. 2004). This might suggest the absence of correlation between the presence of planets and presence of debris disks, but this conclusion may be premature. For instance, the incidences of low-mass planets ("Neptunes"), similar to debris disks, do not seem to correlate with metallicity (Sousa et al. 2008). Also, it is not known if such a correlation exists for more distant planets that cannot be found with the RV techniques. Thus a correlation between the presence of planets and presence of debris disks cannot be ruled out. In fact, there are hints for the debris disk harboring systems with a planet detection to possess brighter, or dustier, disks (thus higher disk detection rates) than systems without a planet detection (Beichman et al. 2005; Trilling et al. 2008; Bryden et al. 2009a).

8 DEBRIS DISKS: THINKING OF PLANETARY SYSTEMS

We now focus on those planetary systems that, like our solar system, are known to contain, apart from the central star and one or more planets, also an outer and/or inner planetesimal belt, or a combination of them. A handful of "full" systems in this sense have been found so far, but only first steps have been taken to elucidate their detailed structure. Examples are Fomalhaut (Kalas et al. 2008), ϵ Eri (Backman et al. 2009), q^1 Eri (Liseau et al. 2008), HR8799 (Reidemeister et al. 2009), HD 38529 (Moro-Martín et al. 2007b), and HD 69830 (Beichman et al. 2005; Lisse et al. 2007; Payne et al. 2009).

As an example, we take the system HR 8799, a nearby A-type star with three directly imaged planetary candidates (Marois et al. 2008), of which the outermost one was recently confirmed by Lafrenière et al. (2009) and by Fukagawa et al. (2009) by analyses of the archival data taken earlier. Apart from the planets, HR 8799 has long been known to harbor cold circumstellar dust responsible for excess emission in the far-IR discovered by IRAS (Sadakane & Nishida 1986; Zuckerman & Song 2004; Rhee et al. 2007). The rather strong IR excess has also been confirmed with ISO/ISOPHOT measurements (Moór et al. 2006), and recently the dust disk was resolved with Spitzer/MIPS at 24 and 70 μm by Su et al. (2009). Additionally, Spitzer/IRS measurements provided evidence of warm dust emission in the mid-IR (Jura et al. 2004; Chen et al. 2006). Both cold and warm dust emission is indicative of two dust-producing planetesimal belts. Reidemeister et al. (2009) undertook a coherent analysis of various observational data for all known components of the system, including the central star, imaged companions, and dust. This has led to a view of a

[1] True fractions are likely much higher. Most recent analysis of the HARPS GTO survey data suggests that $30 \pm 10\%$ of solar-type stars may host close-in (periods < 100 days), low-mass ($< 30 M_\oplus$) planets (Udry et al., paper presented at the ESO/CAUP conference "Towards Other Earths: perspectives and limitations in the ELT era," Porto, Portugal, 19-23 October 2009).

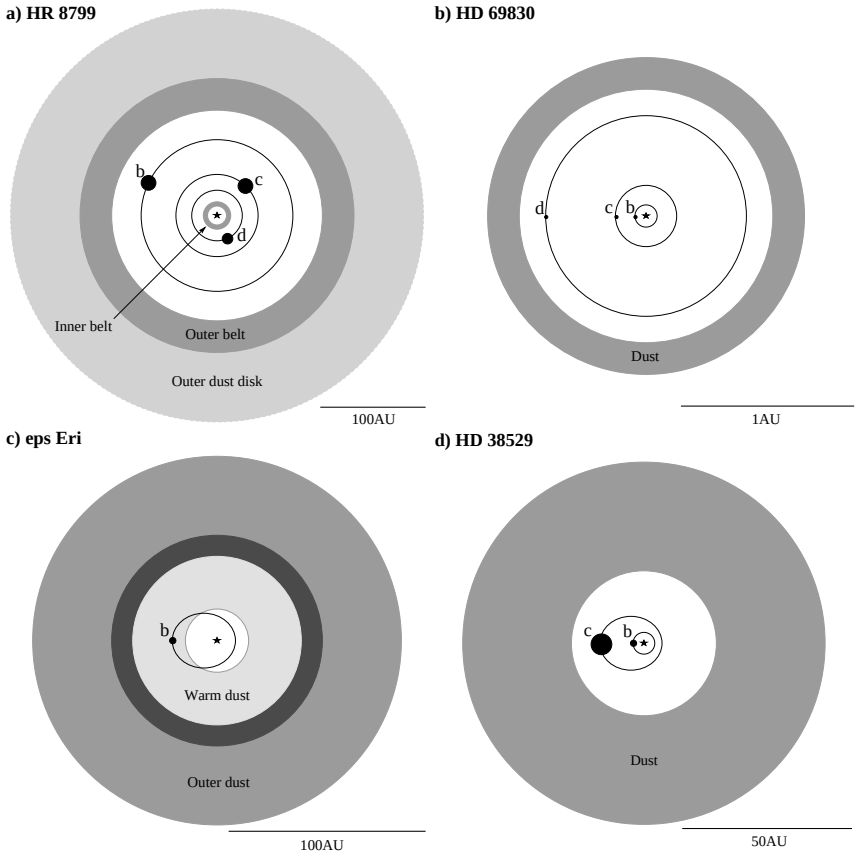

Fig. 7 Schematics of four planetary systems with at least one planet and one planetesimal belt: (a) HR 8799, (b) HD 69830, (c) ϵ Eri, and (d) HD 38529. Only known – not just presumed – components are shown. Sketches are not to scale. Distance rulers roughly reflect the size of the entire systems, and the inner parts of the ϵ Eri and HD 38529 are artificially enlarged. The planets are marked with filled circles whose size is representative of their masses.

complex planetary system with an asteroid-like dust producing an inner belt at $\sim 10\,\mathrm{AU}$, three planets of several Jupiter masses likely locked in a triple Laplace resonance, and an outer Kuiper-like planetesimal belt at $\sim 100\,\mathrm{AU}$ which is associated with a tenuous dust disk that extends to several hundreds of AU from the star. Although many parameters of this system are very different from those of our solar system (young age, luminous central star, very massive planets), the arrangement of these components appears similar (Fig. 7a).

Other "full" planetary systems show less similarity to the solar system. For instance, the system of HD 69830, a nearby $4-10\,\mathrm{Gyr}$ old K0V star, has a very compact configuration with three Neptune-mass planets within $\sim 1\,\mathrm{AU}$ (Lovis et al. 2006) and a "warm" (excess at 8–$35\,\mu\mathrm{m}$) dust belt just exterior to the planetary region (Beichman et al. 2005) (Fig. 7b). A natural guess that dust can be collisionally produced in an asteroid belt analog fails because the dust fractional luminosity is too high (see Sect. 6). Several scenarios have been proposed to explain the origin of the warm emission, but all of them have still unresolved problems (see Payne et al. 2009, for a detailed discussion).

The nearby (3.2 pc), $\lesssim 1$ Gyr old K2 V star ϵ Eridani has a ring of cold dust at ~ 60 AU seen in resolved sub-mm images (Greaves et al. 1998, 2005), which is encompassed by an extended disk of warm dust resolved by Spitzer/MIPS (Backman et al. 2009). The star is orbited by an RV planet (Hatzes et al. 2000; Benedict et al. 2006; Butler et al. 2006) with a semimajor axis of 3.4 AU, and another outer planet is expected to orbit at ~ 40 AU, producing the inner cavity and a clumpy structure in the outer ring (Liou & Zook 1999; Ozernoy et al. 2000; Quillen & Thorndike 2002; Deller & Maddison 2005) (Fig. 7c). The excess emission at $\lambda \gtrsim 15\,\mu$m in a Spitzer/IRS spectrum (Backman et al. 2009) indicates that there is warm dust at just a few AU from the star. Its origin is obscure, as an inner "asteroid belt" that could produce this dust would be destroyed by the known inner planet (Brogi et al. 2009).

One more example of a "full" planetary system is the one around a 3.5 Gyr old G8III/IV star HD 38529 (Moro-Martín et al. 2007b). It hosts two known RV companions with $M \sin i$ of 0.8 and 12.2 Jupiter masses, semimajor axes of $0.13\,$AU and $3.74\,$AU, and eccentricities of 0.25 and 0.35, respectively. Spitzer observations show that HD 38529 has an excess at $70\,\mu$m, which is compatible with dust coming from a "Kuiper belt" between 20–$50\,$AU (Fig. 7d).

We do not yet know which combination of planets and dusty planetesimal belts is common, how these components are typically arranged, and which circumstances are decisive to set one or another type of architecture. However, it is particularly interesting to see how the dust helps to better understand the systems. We take an example of HR 8799 again. First, dust helped to narrow the previously reported range of age estimates of the system, from $30\,$Myr (Rhee et al. 2007) to $\approx 1100\,$Myr (Song et al. 2001). Namely, the measured IR excess ratio of ~ 100 at 60 –90 μm would be typical of a debris disk star of age $\lesssim 50$ Myr (see Su et al. 2006, their fig. 5). Good age estimates are crucial from every point of view, but they also improved the mass estimates of three planets. Indeed, the masses of three planets are estimated from their observed luminosities with the aid of the evolutionary models, and the results strongly depend on the age of the system. Old ages would inevitably imply companion masses in the brown dwarf range, and three companions would then be dynamically unstable, but for the ages of $\lesssim 50$ Myr there are stable solutions (Goździewski & Migaszewski 2009; Reidemeister et al. 2009; Fabrycky & Murray-Clay 2010). Second, the fact that dust in the outer ring was detected as close as at 120 AU from the star and that dust in the inner ring extends to at least 10 AU away from it sets independent upper limits of planetary masses that are consistent with masses from evolutionary models. Third, dust helped to constrain the orientation of the entire system, whose knowledge is needed to convert the sky-projected positions into their true position in space, setting correct initial conditions for the dynamical stability analyses. Reidemeister et al. (2009) showed that stellar rotational velocity is consistent with an inclination of 13° – 30°, whereas $i \gtrsim 20^\circ$ is needed for the system to be dynamically stable, thus arguing for a probable inclination of 20° – 30°. That nearly face-on orientation was confirmed by resolved images of the outer dust disk obtained by Su et al. (2009).

9 OPEN QUESTIONS

After twenty-five years of research on circumstellar debris disks since the first discoveries around Vega (Aumann et al. 1984) and β Pictoris (Smith & Terrile 1984), astronomers can unambiguously place them into the general context of formation and evolution of planetary systems. We know that stars form in collapsing interstellar clouds, that young stars are surrounded by dense, gas- and dust-rich protoplanetary disks in which planets can form, and that debris disks are what remains around the star after the dispersal of that primordial gas at ages of $\sim 10\,$Myr or slightly below. This view is directly supported by the observations that show a clear difference between the disks around younger and older stars. Below those ages, the mass of dust in circumstellar disks retrieved from the IR excesses is typically $\sim 10^2 M_\oplus$ (Earth mass), and above them it drops to below one $\sim 1 M_\oplus$. Applying a standard gas-to-dust ratio of $\sim$ 100:1 to protoplanetary disks, their mass is estimated to

be $\sim 10^4 M_\oplus$, which is consistent with direct gas detections. Direct detection of gas in debris disks is very difficult, and determination of its mass is rather uncertain even where it was detected, but is it likely that the gas mass does not exceed a fraction of the Earth mass even in the most gas-rich debris disks such as β Pic and HD 32297.

One concludes that a certain star possesses a debris disk if thermal emission of circumstellar dust and/or stellar light scattered by it has been detected, and if the amount of dust is below a certain limit, which is taken to be 10^{-2} in terms of the fractional luminosity (Lagrange et al. 2000). The latter is required to distinguish between debris disks and protoplanetary disks. An additional criterion is that the central star should be older than several Myr. From observations, we can only say that dust is present, and from resolved images we know that it is present in the form of a disk rather than an envelope, but a question is where that dust comes from. It is easy to estimate the dust lifetimes around a star against collisions, P-R or stellar wind drag, or destructive processes such as photosputtering. Which removal mechanism is dominant depends on the properties of the central star, dustiness of the disk, and dust composition — but the resulting dust lifetime is usually well below $1\,\mathrm{Myr}$. Since debris disks are commonly observed around stars with ages up to several Gyr, the probability that we are "catching" freshly-born dust is vanishingly low, and so, one or another mechanism to continually replenish the disks is required. There is currently little doubt that the main mechanism that supplies dust is collisions between planetesimals that orbit the host stars of debris disks. Thus the very existence of debris disks is strong evidence for planetesimal populations orbiting a significant fraction of main sequence stars. This, in turn, tells us that planetesimal formation in protoplanetary disks is efficient. However, we do not yet know how these planetesimals typically form. Future debris disk studies may help to discern between alternative mechanisms of planetesimal formation, since they predict different size distributions of planetesimals and/or preferential formation of planetesimals in different regions of protoplanetary disks, which may be reflected in dust emission at the later evolutionary phase of debris disks.

What is the true incidence of debris disks around main-sequence stars? Frequency of detection of protoplanetary disks in clusters younger than $\sim 1\,\mathrm{Myr}$ is almost 100% (Hernández et al. 2007), but the detection fraction of debris disks is $\approx 15\%$ across different spectral types and ages of stars (but $\approx 60\%$ for A-stars at ~ 10 Myr). However, this may only reflect the sensitivity of current observations. It is possible that many other stars, perhaps even 100%, harbor fainter debris disks that yet remain undetectable. The same applies to planets. Current RV detections lead to frequencies of Jupiter-mass planets of $\sim 7\%$, and of lower-mass planets of $\sim 30\%$, but many more — perhaps nearly all — stars may harbor planets that simply escape detection with present-day techniques and instruments. Statistical relations between systems with planets and disks remain unclear. We only know that there are stars that have both. Thus, the typical questions are: Do nearly all mature stars harbor planets, planetesimals, and dust? Are there systems that have planets, but do not have planetesimal belts? Are there systems with planetesimal belts but without planets? Are there systems in which protoplanetary disks failed to produce both?

Accordingly, it is not yet possible to judge the approximate place of our own solar system's planetesimal families, including transneptunian objects, asteroids, and comets, in the menagerie of debris disks in other planetary systems. It is clear that the solar system's dust disk, dominated by dust in the Kuiper belt region, is by orders of magnitude fainter than known debris disks of other stars. However, it is not yet clear why, and, due to current observational limitations, it is not yet known if any other stars possess disks as tenuous as ours. Also, if they do, what is more common — brighter or fainter disks?

We saw that statistics of IR excesses of hundreds of debris disk stars and their evolution with a system's age, as well as observed SEDs and resolved images of some of the brightest debris disks appear consistent with a standard collisional evolution scenario. It implies one (or more) planetesimal belt with a steady-state cascade of successive collisions that grinds the planetesimals all the way down to dust, and whose distribution is then shaped by gravity and radiation pressure forces. In such

systems, steady-state collisional models place useful, albeit often weak, constraints on size and spatial distributions of planetesimals, their dynamical excitation, and mechanical strength. However, it remains unclear what mechanism stirs planetesimals to the extent that allows the collisional cascade to operate. Are these largest, Pluto-sized planetesimals embedded in the disks, neighboring planets, or both? On the other hand, there are systems – or their parts – that are certainly not consistent with a steady-state collisional evolution. These are exemplified by systems with substantial "hot" dust emission in the mid-IR, such as HD 69830 and η Crv, and by systems with "exozodiacal" dust within $\sim 1\,\mathrm{AU}$ from the star. Here, there is too much dust to be explained with dust produced locally in a steady-state collisional cascade. It remains unclear whether non-collisional mechanisms such as sublimation, one-time major collisions, or non-local production in outer belts with subsequent inward transport are at work in such systems.

Further open questions are related to the disk structure. Most, if not all, known debris disks have inner cavities suggesting that planetesimals are not present there. Nonetheless, it is not known whether the lack of planetesimals is because they originally fail to form there or were removed by planets later. Interpretation of azimuthal and vertical structures such as clumps, spirals, warps, and wing asymmetries remains ambiguous, too. They can be naturally explained by gravitational interactions of solids with planets, but many can equally well be attributed to "non-planetary" mechanisms such as major collisional break-ups, stellar flybys, or interaction with the surrounding interstellar gas and dust.

We finally note that detailed studies of thermal emission of debris dust, notably the analyses of high-resolution mid- and far-IR spectra, offer a unique way to probe chemical composition of dust and its parent planetesimals. Only the first steps have been taken in this direction. For instance it is not yet clear, why some of the disks reveal spectral features and some others do not, to which extent the inferred composition of dust reflects that of its parent planetesimals, and whether the dissimilarity of the observed spectra traces back to different chemical evolution and mixing scenarios at the preceding, protoplanetary disk stage. Additional information can also be gained by analysis of gas in young debris disks, which is thought to be a product of dust grain disintegration by various mechanisms.

Future observations and modeling work should give answers to these and other questions. On any account, debris disks must be treated as an important constituent part of planetary systems, and there is little doubt that they can serve as tracers of planetesimals and planets and shed light on the planetesimal and planet formation processes. Thus the lesson for planetary system research is: "follow the dust."

Acknowledgements This paper is based on the lecture given at the 1st CPS International School of Planetary Sciences held in Kobe, Japan, on January 5–9, 2009, and I wish to thank the organizers for the invitation and support. This review has further benefited from the author's participation in the program "Dynamics of Discs and Planets," organized by the Isaac Newton Institute for Mathematical Sciences in Cambridge. I thank Torsten Löhne, Hiroshi Kobayashi, Sebastian Müller, Martin Reidemeister, and Christian Vitense for stimulating discussions and Sebastian Müller for assistance in preparing the figures. A speedy and careful review by an anonymous referee helped to improve the paper. Support by the German Research Foundation (*Deutsche Forschungsgemeinschaft, DFG*), project number Kr 2164/8–1, by the *Deutscher Akademischer Austauschdienst (DAAD)*, project D/0707543, and by the International Space Science Institute in Bern, Switzerland ("Exozodiacal Dust Disks and Darwin" working group, *http://www.issibern.ch/teams/exodust/*) is acknowledged.

References

Absil, O., di Folco, E., Mérand, A., et al. 2006, A&A, 452, 237
Absil, O., di Folco, E., Mérand, A., et al. 2008, A&A, 487, 1041
Akeson, R. L., Ciardi, D. R., Millan-Gabet, R., et al. 2009, ApJ, 691, 1896
Alexander, R. 2008, New Astronomy Review, 52, 60
Apai, D., Janson, M., Moro-Martín, A., et al. 2008, ApJ, 672, 1196
Ardila, D. R., Golimowski, D. A., Krist, J. E., et al. 2004, ApJ, 617, L147
Artymowicz, P. 1997, Ann. Rev. Earth Planet. Sci., 25, 175
Artymowicz, P., & Clampin, M. 1997, ApJ, 490, 863
Aufdenberg, J. P., Mérand, A., Coudé du Foresto, V., et al. 2006, ApJ, 645, 664
Augereau, J., & Beust, H. 2006, A&A, 455, 987
Augereau, J.-C., Nelson, R. P., Lagrange, A.-M., et al. 2001, A&A, 370, 447
Aumann, H. H., Beichman, C. A., Gillett, F. C., et al. 1984, ApJ, 278, L23
Backman, D., Marengo, M., Stapelfeldt, K., et al. 2009, ApJ, 690, 1522
Barge, P., Pellat, R., & Millet, J. 1982, A&A, 115, 8
Beichman, C. A., Bryden, G., Gautier, T. N., et al. 2005, ApJ, 626, 1061
Beichman, C. A., Bryden, G., Rieke, G. H., et al. 2005, ApJ, 622, 1160
Beichman, C. A., Bryden, G., Stapelfeldt, K. R., et al. 2006, ApJ, 652, 1674
Benedict, G. F., McArthur, B. E., Gatewood, G., et al. 2006, AJ, 132, 2206
Benz, W., & Asphaug, E. 1999, Icarus, 142, 5
Beust, H., & Valiron, P. 2007, A&A, 466, 201
Blum, J., & Wurm, G. 2008, ARA&A, 46, 21
Boltzmann, L. 1896, Vorlesungen über Gastheorie (J.A. Barth, Leipzig)
Booth, M., Wyatt, M. C., Morbidelli, A., Moro-Martín, A., & Levison, H. F. 2009, MNRAS, 399, 385
Brauer, F., Dullemond, C. P., Johansen, A., et al. 2007, A&A, 469, 1169
Breiter, S., & Jackson, A. A. 1998, MNRAS, 299, 237
Brogi, M., Marzari, F., & Paolicchi, P. 2009, A&A, 499, L13
Bromley, B. C., & Kenyon, S. J. 2006, AJ, 131, 2737
Bryden, G., Beichman, C. A., Carpenter, J. M., et al. 2009a, ApJ, 705, 1226
Bryden, G., Beichman, C. A., Trilling, D. E., et al. 2006, ApJ, 636, 1098
Bryden, G., Stapelfeldt, K., Dowell, C. D., et al. 2009b, BAAS, 41, 209, abstract
Burns, J. A., Lamy, P. L., & Soter, S. 1979, Icarus, 40, 1
Butler, R. P., Wright, J. T., Marcy, G. W., et al. 2006, ApJ, 646, 505
Carpenter, J. M., Bouwman, J., Mamajek, E. E., et al. 2009, ApJS, 181, 197
Chandrasekhar, S. 1943, Rev. Mod. Phys., 15, 1
Chapman, S., & Cowling, T. G. 1970, The Mathematical Theory of Nonuniform Gases (New York: Cambridge Univ. Press)
Chen, C. H., Fitzgerald, M. P., & Smith, P. S. 2008, ApJ, 689, 539
Chen, C. H., Li, A., Bohac, C., et al. 2007, ApJ, 666, 466
Chen, C. H., Sargent, B. A., Bohac, C., et al. 2006, ApJS, 166, 351
Consolmagno, G. 1980, Icarus, 43, 203
Czechowski, A., & Mann, I. 2007, ApJ, 660, 1541
Davis, D. R., Chapman, C. R., Weidenschilling, S. J., & Greenberg, R. 1985, Icarus, 62, 30
Debes, J. H., Weinberger, A. J., & Kuchner, M. J. 2009, ApJ, 702, 318
Deller, A. T., & Maddison, S. T. 2005, ApJ, 625, 398
Dell'Oro, A., Marzari, F., Paolicchi, P., & Vanzani, V. 2001, A&A, 366, 1053
Dell'Oro, A., Marzari, P. P. F., Dotto, E., & Vanzani, V. 1998, A&A, 339, 272
Dell'Oro, A., & Paolicchi, P. 1998, Icarus, 136, 328

Dell'Oro, A., Paolicchi, P., Cellino, A., & Zappalà, V. 2002, Icarus, 156, 191
Di Folco, E., Absil, O., Augereau, J.-C., et al. 2007, A&A, 475, 243
Di Folco, E., Thévenin, F., Kervella, P., et al. 2004, A&A, 426, 601
Dohnanyi, J. S. 1969, J. Geophys. Res., 74, 2531
Dominik, C., & Decin, G. 2003, ApJ, 598, 626
Durda, D. D., & Dermott, S. F. 1997, Icarus, 130, 140
Durda, D. D., Greenberg, R., & Jedicke, R. 1998, Icarus, 135, 431
Faber, P., & Quillen, A. C. 2007, MNRAS, 382, 1823
Fabrycky, D. C., & Murray-Clay, R. A. 2010, ApJ, 710, 1408
Ferlet, R., Vidal-Madjar, A., & Hobbs, L. M. 1987, A&A, 185, 267
Fitzgerald, M. P., Kalas, P. G., & Graham, J. R. 2007, ApJ, 670, 557
Fitzgerald, M. P., Kalas, P. G., & Graham, J. R. 2009, ApJ, 706, L41
Freistetter, F., Krivov, A. V., & Löhne, T. 2007, A&A, 466, 389
Fukagawa, M., Itoh, Y., Tamura, M., et al. 2009, ApJ, 696, L1
Gautier, T. N., III, Rieke, G. H., Stansberry, J., et al. 2007, ApJ, 667, 527
Gledhill, T. M., Scarrott, S. M., & Wolstencroft, R. D. 1991, MNRAS, 252, 50
Goldreich, P., Lithwick, Y., & Sari, R. 2004, ARA&A, 42, 549
Gomes, R., Levison, H. F., Tsiganis, K., & Morbidelli, A. 2005, Nature, 435, 466
Gorlova, N., Rieke, G. H., Muzerolle, J., et al. 2006, ApJ, 659, 1028
Goździewski, K., & Migaszewski, C. 2009, MNRAS, 397, L16
Graham, J. R., Kalas, P. G., & Matthews, B. C. 2007, ApJ, 654, 595
Greaves, J. S. 2005, Science, 307, 68
Greaves, J. S., Fischer, D. A., & Wyatt, M. C. 2006, MNRAS, 366, 283
Greaves, J. S., Holland, W. S., Jayawardhana, R., Wyatt, M. C., & Dent, W. R. F. 2004, MNRAS, 348, 1097
Greaves, J. S., Holland, W. S., Moriarty-Schieven, G., et al. 1998, A&A, 506, L133
Greaves, J. S., Holland, W. S., Wyatt, M. C., et al. 2005, ApJ, 619, L187
Greaves, J. S., & Wyatt, M. C. 2003, MNRAS, 345, 1212
Greaves, J. S., Wyatt, M. C., Holland, W. S., & Dent, W. R. F. 2004, MNRAS, 351, L54
Grigorieva, A., Artymowicz, P., & Thébault, P. 2007, A&A, 461, 537
Grün, E., Gustafson, B. A. S., Dermott, S., & Fechtig, H. 2001, Interplanetary Dust (Springer), 804
Grün, E., Zook, H. A., Fechtig, H., & Giese, R. H. 1985, Icarus, 62, 244
Hatzes, A. P., Cochran, W. D., McArthur, B., et al. 2000, ApJ, 544, L145
Heng, K., & Keeton, C. R. 2009, ApJ, 707, 621
Hernández, J., Briceño, C., Calvet, N., et al. 2006, ApJ, 652, 472
Hernández, J., Hartmann, L., Megeath, T., et al. 2007, ApJ, 662, 1067
Hillenbrand, L. A. 2008, Physica Scripta Volume T, 130, 014024
Hillenbrand, L. A., Carpenter, J. M., Kim, J. S., et al. 2008, ApJ, 677, 630
Holland, W. S., Greaves, J. S., Zuckerman, B., et al. 1998, Nature, 392, 788
Holsapple, K. A. 1994, Planet. Space Sci., 42, 1067
Itoh, Y., Oasa, Y., & Fukagawa, M. 2006, ApJ, 652, 1729
Janson, M., Brandner, W., Henning, T., et al. 2007, AJ, 133, 2442
Janson, M., Reffert, S., Brandner, W., et al. 2008, A&A, 488, 771
Johansen, A., Klahr, H., & Henning, T. 2006, ApJ, 636, 1121
Johansen, A., Oishi, J. S., Low, M.-M. M., et al. 2007, Nature, 448, 1022
Jura, M., Chen, C. H., Furlan, E., et al. 2004, ApJS, 154, 453
Kalas, P. 2005, ApJ, 635, L169
Kalas, P., Fitzgerald, M. P., & Graham, J. R. 2007, ApJ, 661, L85
Kalas, P., Graham, J. R., Chiang, E., et al. 2008, Science, 322, 1345

Kalas, P., Graham, J. R., Clampin, M. C., & Fitzgerald, M. P. 2006, ApJ, 637, L57
Kalas, P., Liu, M. C., & Matthews, B. C. 2004, Science, 303, 1990
Kapišinský, I. 1984, Contrib. Astron. Observ. Scalnaté Pleso, 12, 99
Kennedy, G. M., & Wyatt, M. C. 2009, MNRAS, submitted
Kenyon, S. J., & Bromley, B. C. 2002, AJ, 123, 1757
Kenyon, S. J., & Bromley, B. C. 2004a, AJ, 127, 513
Kenyon, S. J., & Bromley, B. C. 2004b, ApJ, 602, L133
Kenyon, S. J., & Bromley, B. C. 2004c, AJ, 128, 1916
Kenyon, S. J., & Bromley, B. C. 2008, ApJS, 179, 451
Kenyon, S. J., & Luu, J. X. 1998, AJ, 115, 2136
Kenyon, S. J., & Luu, J. X. 1999a, AJ, 118, 1101
Kenyon, S. J., & Luu, J. X. 1999b, ApJ, 526, 465
Kim, J. S., Hines, D. C., Backman, D. E., et al. 2005, ApJ, 632, 659
Kimura, H., Ishimoto, H., & Mukai, T. 1997, A&A, 326, 263
Kobayashi, H., Watanabe, S., Kimura, H., & Yamamoto, T. 2009, Icarus, 201, 395
Kóspál, Á., Ardila, D. R., Moór, A., & Ábrahám, P. 2009, ApJ, 700, L73
Krivov, A. V., Herrmann, F., Brandeker, A., & Thébault, P. 2009, A&A, 507, 1503
Krivov, A. V., Kimura, H., & Mann, I. 1998, Icarus, 134, 311
Krivov, A. V., Löhne, T., & Sremčević, M. 2006, A&A, 455, 509
Krivov, A. V., Mann, I., & Krivova, N. A. 2000, A&A, 362, 1127
Krivov, A. V., Müller, S., Löhne, T., & Mutschke, H. 2008, ApJ, 687, 608
Krivov, A. V., Queck, M., Löhne, T., & Sremčević, M. 2007, A&A, 462, 199
Krivov, A. V., Sremčević, M., & Spahn, F. 2005, Icarus, 174, 105
Krivova, N. A., Krivov, A. V., & Mann, I. 2000, ApJ, 539, 424
Lafrenière, D., Marois, C., Doyon, R., & Barman, T. 2009, ApJ, 694, L148
Lagrange, A.-M., Backman, D. E., & Artymowicz, P. 2000, in Protostars and Planets IV, eds. V. Mannings, A. P. Boss, & S. S. Russell (Tucson: University of Arizona Press), 639
Lagrange, A.-M., Gratadour, D., Chauvin, G., et al. 2009, A&A, 493, L21
Laor, A., & Draine, B. T. 1993, ApJ, 402, 441
Lawler, S. M., Beichman, C. A., Bryden, G., et al. 2009, ApJ, 705, 89
Lecavelier des Etangs, A., Scholl, H., Roques, F., Sicardy, B., & Vidal-Madjar, A. 1996, Icarus, 123, 168
Lestrade, J.-F., Wyatt, M. C., Bertoldi, F., Dent, W. R. F., & Menten, K. M. 2006, A&A, 460, 733
Liou, J.-C., & Zook, H. A. 1999, AJ, 118, 580
Liseau, R., Risacher, C., Brandeker, A., et al. 2008, A&A, 480, L47
Lissauer, J. J. 1987, Icarus, 69, 249
Lisse, C. M., Beichman, C. A., Bryden, G., & Wyatt, M. C. 2007, ApJ, 658, 584
Lisse, C. M., Chen, C. H., Wyatt, M. C., & Morlok, A. 2008, ApJ, 673, 1106
Lisse, C. M., Chen, C. H., Wyatt, M. C., et al. 2009, ApJ, 701, 2019
Liu, M. C., Matthews, B. C., Williams, J. P., & Kalas, P. G. 2004, ApJ, 608, 526
Löhne, T., Krivov, A. V., & Rodmann, J. 2008, ApJ, 673, 1123
Lovis, C., Mayor, M., Pepe, F., et al. 2006, Nature, 441, 305
Marengo, M., Megeath, S. T., Fazio, G. G., et al. 2006, ApJ, 647, 1437
Marois, C., Macintosh, B., Barman, T., et al. 2008, Science, 322, 1348
Marsh, K. A., Dowell, C. D., Velusamy, T., Grogan, K., & Beichman, C. A. 2006, ApJ, 646, L77
Matthews, B. C., Greaves, J. S., Holland, W. S., et al. 2007, PASP, 119, 842
Meyer, M. R., Carpenter, J. M., Mamajek, E. E., et al. 2008, ApJ, 673, L181
Meyer, M. R., Hillenbrand, L. A., Backman, D. E., et al. 2004, ApJS, 154, 422
Moerchen, M. M., Telesco, C. M., Packham, C., & Kehoe, T. J. J. 2007, ApJ, 655, L109

Moór, A., Ábrahám, P., Derekas, A., et al. 2006, ApJ, 644, 525
Morfill, G. E., & Grün, E. 1979, Planet. Space Sci., 27, 1269
Moro-Martín, A., Carpenter, J. M., Meyer, M. R., et al. 2007a, ApJ, 658, 1312
Moro-Martín, A., & Malhotra, R. 2002, AJ, 124, 2305
Moro-Martín, A., Malhotra, R., Carpenter, J. M., et al. 2007b, ApJ, 668, 1165
Moro-Martín, A., Wyatt, M. C., Malhotra, R., & Trilling, D. E. 2007, Extra-Solar Kuiper Belt Dust Disks, arXiv:astro-ph/0703383
Mouillet, D., Larwood, J. D., Papaloizou, J. B., & Lagrange, A.-M. 1997, MNRAS, 292, 896
Müller, S., Löhne, T., & Krivov, A. V. 2010, ApJ, 708, 1728
Mustill, A. J., & Wyatt, M. C. 2009, MNRAS, 399, 1403
Najita, J., & Williams, J. P. 2005, ApJ, 635, 625
Olofsson, G., Liseau, R., & Brandeker, A. 2001, ApJ, 563, L77
Ortega, V. G., de la Reza, R., Jilinski, E., & Bazzanella, B. 2002, ApJ, 575, L75
Ozernoy, L. M., Gorkavyi, N. N., Mather, J. C., & Taidakova, T. A. 2000, ApJ, 537, L147
Paolicchi, P., Verlicchi, A., & Cellino, A. 1996, Icarus, 121, 126
Payne, M. J., Ford, E. B., Wyatt, M. C., & Booth, M. 2009, MNRAS, 393, 1219
Peterson, D. M., Hummel, C. A., Pauls, T. A., et al. 2006, Nature, 440, 896
Plavchan, P., Jura, M., & Lipscy, S. J. 2005, ApJ, 631, 1161
Plavchan, P., Werner, M. W., Chen, C. H., et al. 2009, ApJ, 698, 1068
Quillen, A. C., & Thorndike, S. 2002, ApJ, 578, L149
Quinn, T., Tremaine, S., & Duncan, M. 1990, ApJ, 355, 667
Raymond, S. N., Armitage, P. J., & Gorelick, N. 2009, ApJ, 699, L88
Redfield, S. 2007, ApJ, 656, L97
Reidemeister, M., Krivov, A. V., Schmidt, T. O. B., et al. 2009, A&A, 503, 247
Rhee, J. H., Song, I., & Zuckerman, B. 2008, ApJ, 675, 777
Rhee, J. H., Song, I., Zuckerman, B., & McElwain, M. 2007, ApJ, 660, 1556
Rice, W. K. M., Lodato, G., Pringle, J. E., Armitage, P. J., & Bonnell, I. A. 2006, MNRAS, 372, L9
Rieke, G. H., Su, K. Y. L., Stansberry, J. A., et al. 2005, ApJ, 620, 1010
Sadakane, K., & Nishida, M. 1986, PASP, 98, 685
Safronov, V. S. 1969, Evolution of the Protoplanetary Cloud and Formation of the Earth and Planets (Moscow (in Russian): Nauka) [English translation: NASA TTF-677, 1972.]
Schütz, O., Meeus, G., & Sterzik, M. F. 2005, A&A, 431, 175
Sheret, I., Dent, W. R. F., & Wyatt, M. C. 2004, MNRAS, 348, 1282
Siegler, N., Muzerolle, J., Young, E. T., et al. 2007, ApJ, 654, 580
Smith, B. A., & Terrile, R. I. 1984, Science, 226, 1421
Smoluchowski, M. V. 1916, Zeitschrift für Physik, 17, 557
Song, I., Caillault, J.-P., Barrado y Navascués, D., & Stauffer, J. R. 2001, ApJ, 546, 352
Sousa, S. G., Santos, N. C., Mayor, M., et al. 2008, A&A, 487, 373
Spaute, D., Weidenschilling, S. J., Davis, D. R., & Marzari, F. 1991, Icarus, 92, 147
Stapelfeldt, K. R., Holmes, E. K., Chen, C., et al. 2004, ApJS, 154, 458
Stark, C. C., & Kuchner, M. J. 2009, ApJ, 707, 543
Stark, C. C., Kuchner, M. J., Traub, W. A., et al. 2009, ApJ, 703, 1188
Stewart, S. T., & Leinhardt, Z. M. 2009, ApJ, 691, L133
Strubbe, L. E., & Chiang, E. I. 2006, ApJ, 648, 652
Su, K. Y. L., Rieke, G. H., Misselt, K. A., et al. 2005, ApJ, 628, 487
Su, K. Y. L., Rieke, G. H., Stansberry, J. A., et al. 2006, ApJ, 653, 675
Su, K. Y. L., Rieke, G. H., Stapelfeldt, K. R., et al. 2009, ApJ, 705, 314
Tamanai, A., Mutschke, H., Blum, J., & Meeus, G. 2006, ApJ, 648, L147

Thébault, P., & Augereau, J.-C. 2005, A&A, 437, 141
Thébault, P., & Augereau, J.-C. 2007, A&A, 472, 169
Thébault, P., & Wu, Y. 2008, A&A, 481, 713
Thébault, P., Augereau, J.-C., & Beust, H. 2003, A&A, 408, 775
Trilling, D. E., Bryden, G., Beichman, C. A., et al. 2008, ApJ, 674, 1086
Trilling, D. E., Stansberry, J. A., Stapelfeldt, K. R., et al. 2007, ApJ, 658, 1289
Udry, S., & Santos, N. C. 2007, ARA&A, 45, 397
Vitense, C., Krivov, A. V., & Löhne, T. 2010, A&A, submitted
Wallis, M. K., & Hassan, M. H. A. 1985, A&A, 151, 435
Weidenschilling, S. J. 1977, MNRAS, 180, 57
Weidenschilling, S. J., Spaute, D., Davis, D. R., Marzari, F., & Ohtsuki, K. 1997, Icarus, 128, 429
Wetherill, G. W. 1980, ARA&A, 18, 77
Williams, J. P., Najita, J., Liu, M. C., et al. 2004, ApJ, 604, 414
Wolf, S., & Hillenbrand, L. A. 2003, ApJ, 596, 603
Wolf, S., & Hillenbrand, L. A. 2005, Comp. Phys. Comm., 171, 208
Wolstencroft, R. D., Scarrott, S. M., & Gledhill, T. M. 1995, Astrophys. Space Sci., 224, 395
Wright, J. T., Marcy, G. W., Butler, R. P., & Vogt, S. S. 2004, ApJS, 152, 261
Wyatt, M. C. 2003, ApJ, 598, 1321
Wyatt, M. C. 2005, A&A, 433, 1007
Wyatt, M. C. 2005, A&A, 440, 937
Wyatt, M. C. 2006, ApJ, 639, 1153
Wyatt, M. C. 2008, ARA&A, 46, 339
Wyatt, M. C., Booth, M., Payne, M. J., & Churcher, L. J. 2010, MNRAS, 402, 657
Wyatt, M. C., Dermott, S. F., Telesco, C. M., et al. 1999, ApJ, 527, 918
Wyatt, M. C., Greaves, J. S., Dent, W. R. F., & Coulson, I. M. 2005, ApJ, 620, 492
Wyatt, M. C., Smith, R., Greaves, J. S., et al. 2007a, ApJ, 658, 569
Wyatt, M. C., Smith, R., Su, K. Y. L., et al. 2007b, ApJ, 663, 365
Wyatt, S. P., & Whipple, F. L. 1950, ApJ, 111, 134
Zook, H. A., & Berg, O. E. 1975, Planet. Space Sci., 23, 183
Zuckerman, B., & Song, I. 2004, ApJ, 603, 738
Zuckerman, B., Song, I., Bessell, M. S., & Webb, R. A. 2001, ApJ, 562, L87